DEVELOPMENT OF A REAL-TIME, MICROPROCESSOR BASED, DETECTOR OF
EPILEPTIFORM ACTIVITY IN EEG

by

LAWRENCE PATRICK PANYCH

B.A., University Of Alberta, 1973
B.Eng. McGill University, 1979

A THESIS SUBMITTED IN PARTIAL FULFILMENT OF

THE REQUIREMENTS FOR THE DEGREE OF

MASTER OF APPLIED SCIENCES

in

THE FACULTY OF GRADUATE STUDIES

Electrical Engineering

We accept this thesis as conforming

to the required standard

THE UNIVERSITY OF BRITISH COLUMBIA

October 1983

Department of Electrical Engineering

The University of British Columbia
2075 Wesbrook Place
Vancouver, Canada
V6T 1W5

Date 15 November 1983

Abstract

This is an experimental thesis describing the development of a monitor for the detection of epileptic activity in the human EEG. The monitor, built around an Apple II Plus microcomputer system, has the capability for real-time detection of seizure activity and interictal transients (spikes and sharp waves or SSW) on 16 EEG channels. A dynamic graphics display symbolically presents to the user a running sum of the SSW detected during a monitoring session. A report is produced at the end of the session which includes a summary of SSW detections and the on-line phase reversal processing of the transients. An automatic seizure detection by the monitor will trigger the marking of the location of seizure records on magnetic EEG recording devices.

Of significance is a theoretical explanation which shows why a simple slope detector performs as well as a complicated parametric transient detector. The real-time capability of the slope detector makes it superior in practical applications. Statistical detection theory is applied to the problem of EEG epileptic transient detection and the computer model which calculates a theoretical performance factor for detectors is described. Simple algorithms for selecting epileptic transients based on morphological considerations and methods of artifact rejection are presented.

The monitor was evaluated in a clinical seizure investigation unit at the University of British Columbia.

Clinically significant seizures were detected over a six month period with a very high success rate. In the cases of patients with focal epilepsies, predictions of focus locations by the device agreed with the neurological diagnoses of the patients.

Table of Contents

List of Tables

List of Figures

Acknowledgement

I. INTRODUCTION

According to the U.S. National Institute of Neurological and Communicative Diseases and Stroke, an estimated 2% of the population suffers from some form of epilepsy.[39] In Canada, this represents about 1/2 million people or close to 50,000 in British Columbia. Most of these people are able to lead productive lives with effective use of medication. For about 20%, however, their condition requires they be given special care, often leading to institutionalization. Fortunately, some of these individuals are candidates for a special curative surgery which can help them to lead normal lives. Before such surgery can be performed an in-depth assessment must be performed requiring extensive patient monitoring.

Monitoring patients with epilepsy is the task of a new Seizure Investigation Unit, recently installed in the Acute Care Hospital at the Health Sciences Center of the University of British Columbia (see figure 1). Patients admitted to the unit are those who have not responded well to medication and for whom surgery is indicated. The seizure unit at the UBC hospital has the capability for monitoring two patients concurrently, around the clock. Patients' movements are monitored by video cameras and electrical signals recorded at the scalp (electroencephalogram or EEG) are registered on special paper chart recorders for viewing (figure 2). Both video and EEG signals are stored on magnetic tape(figure 3).

A neurological diagnosis follows from a study of the video tapes of patient movement during seizure, as well as from EEG tracings of seizure and between-seizure (or interictal) activity. As a prelude to surgery, a goal of the diagnosis is to determine if an epileptic focus exists, how many there are, and where they are.

The recording of seizure or interictal activity is of no use if the medical staff does not know that it is there. Thus, patient monitoring requires intelligent supervision for it to be effective. Most interictal activity goes unnoticed because of the impossibility of reviewing all data. Many seizures are missed because no one is available to make a note of them. The patient has a special push button to press when a seizure occurs. This causes a 10hz signal to be recorded along with the EEG so that when the tape is rewound at high speed there is an audible tone at the location on the tape where the seizure occurred and seizure records are easily obtained. Unfortunately, seizures are often missed because the patient fails to press the (seizure) button.

We are developing a microprocessor-based EEG processor for use in the seizure unit. It detects seizures automatically from patient EEG and signals their occurrence. A computer seizure detection causes the recording tape to be marked as though the seizure button had been pressed. Soon, with the completion of a new video tape machine controller being developed at UBC, when the computer detects a seizure, its video record will be

automatically transferred to a single master tape for easy viewing at a later time.

The EEG processor analyses activity between seizures to detect epileptiform transients known as spikes and sharp waves (SSW's). Statistics of SSW detections are kept and reported at the end of a recording session. The automatic SSW detection can be used to control the EEG recording devices to produce a compressed interictal record.
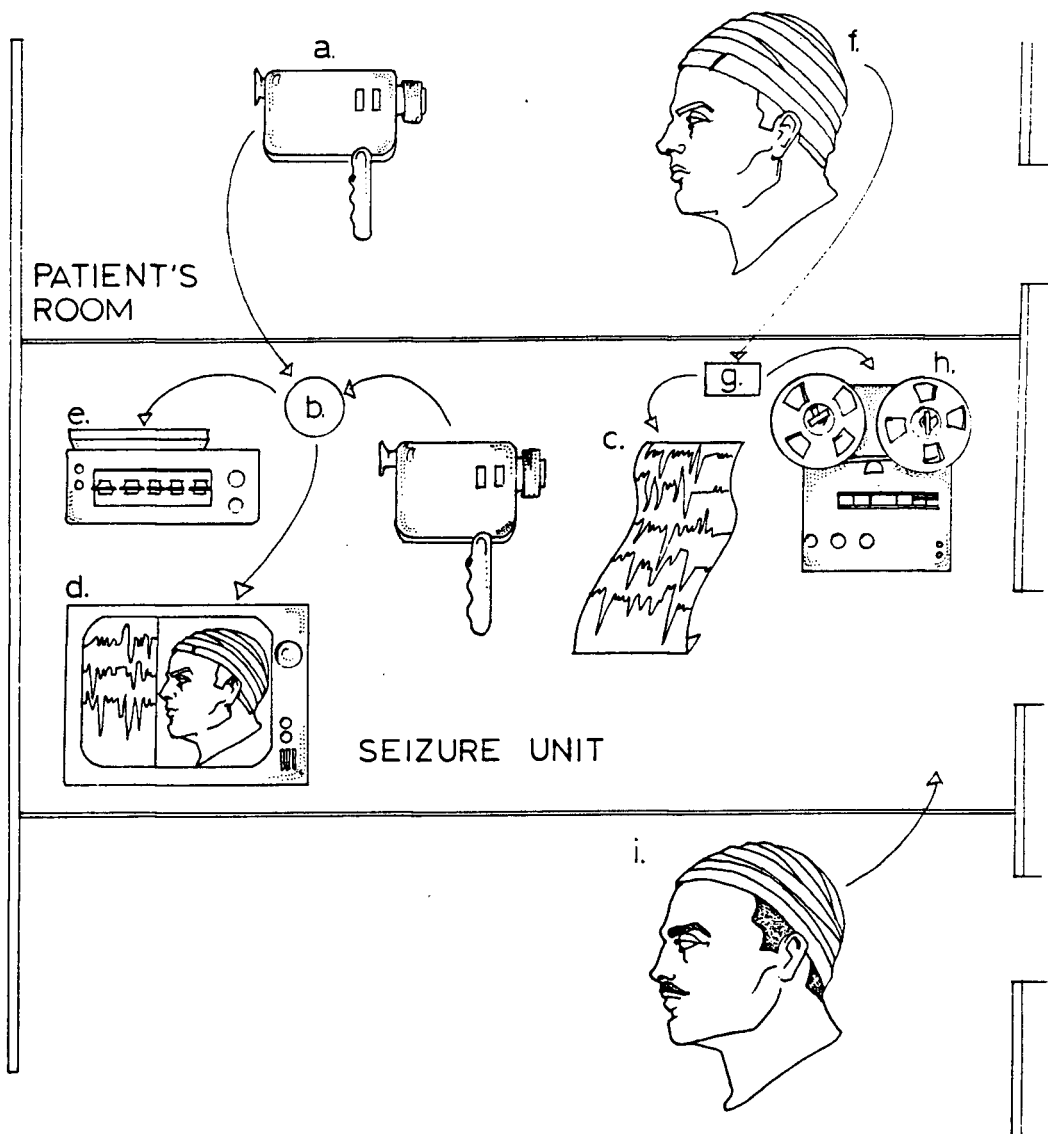
Figure 1 Seizure Investigation Unit. Patient movement is monitored by a video camera(a) and mixed(b) with the video image of the EEG recording(c) to obtain a split screen image(d). The image is then taped(e). Sixteen channels of EEG is recorded(f), multiplexed, and sent via telemetry to the Seizure Unit(g). The multiplexed signal is stored on audio tape(h). A second patient(i) can be monitored at the same time.
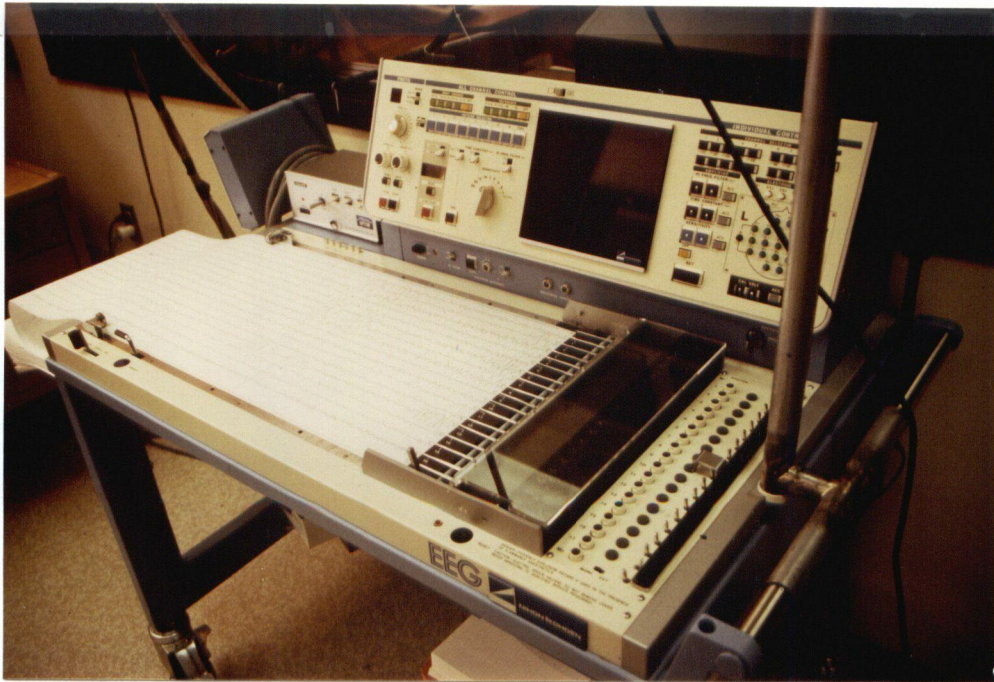
Figure 2 EEG Chart Recorder. A hardcopy of the EEG is obtained
from a Nihon-Kohden chart recorder.

Figure 3 Tape Recording Equipment. Twenty-four hours of EEG is saved using TEAC audio recorders. The last 4 hours of the patient video record is stored on Panasonic video tape recorders.

II. HUMAN EEG AND ITS ANALYSIS

2.1 Origins And Characteristics Of EEG

As early as 1875 Caton discovered that the brain produced electrical activity but the first recorded measurement of potentials at the human scalp was by Berger in 1924. These potentials have since been known as electroencephalograms (EEG) as opposed to electrocortiograms (ECoG) which are recorded at the cortical surface.

EEG potentials originate from a summation of the individual neurons of the brain.[38] Intracellular recordings indicate that the source can be traced to graded synaptic potentials generated by the pyramidal cells of the cerebral cortex.[8] The potentials are attenuated and diffused when conducted through the cerebrospinal fluid, the skull, and the scalp. They are normally less than 100 microvolts in amplitude but may be as high as 1 millivolt.

Scalp potentials are amplified by differential amplifiers with input impedances of 1 to 10 megohms and Common Mode Rejection Ratio in excess of 500 to 1.[7] Single order low and high pass filters (corner frequencies at 70hz and 1hz) are inserted to reduce artifact. Electrodes are placed according to the international 10-20 system (figures 4a and 4b). Recording may be either bipolar (difference of adjacent electrodes) or unipolar (with respect to a reference lead placed on the nose or

occipital bone), although, bipolar recording is favored for its lower sensitivity to noise. Many bipolar interconnection montages (figure 5) are possible.
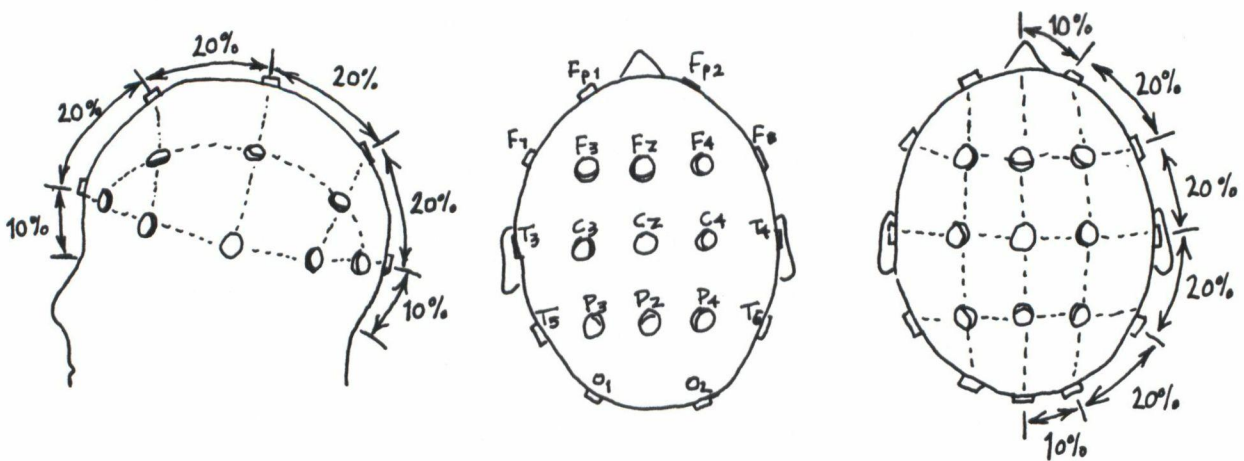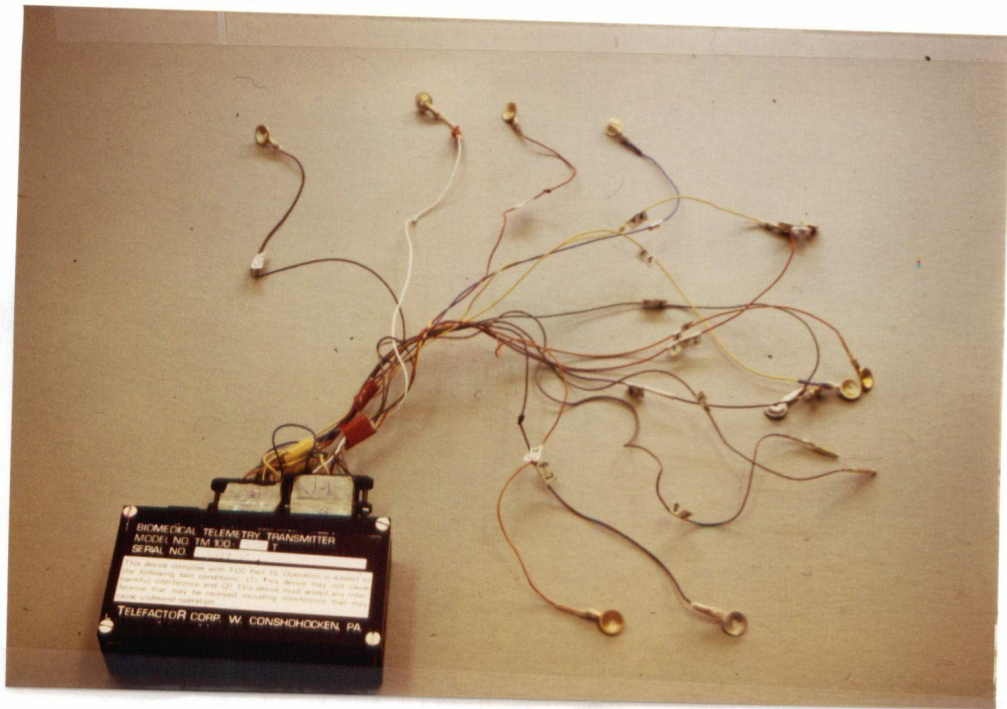
Figure 4 (a)EEG electrodes (b)International 10-20 system.
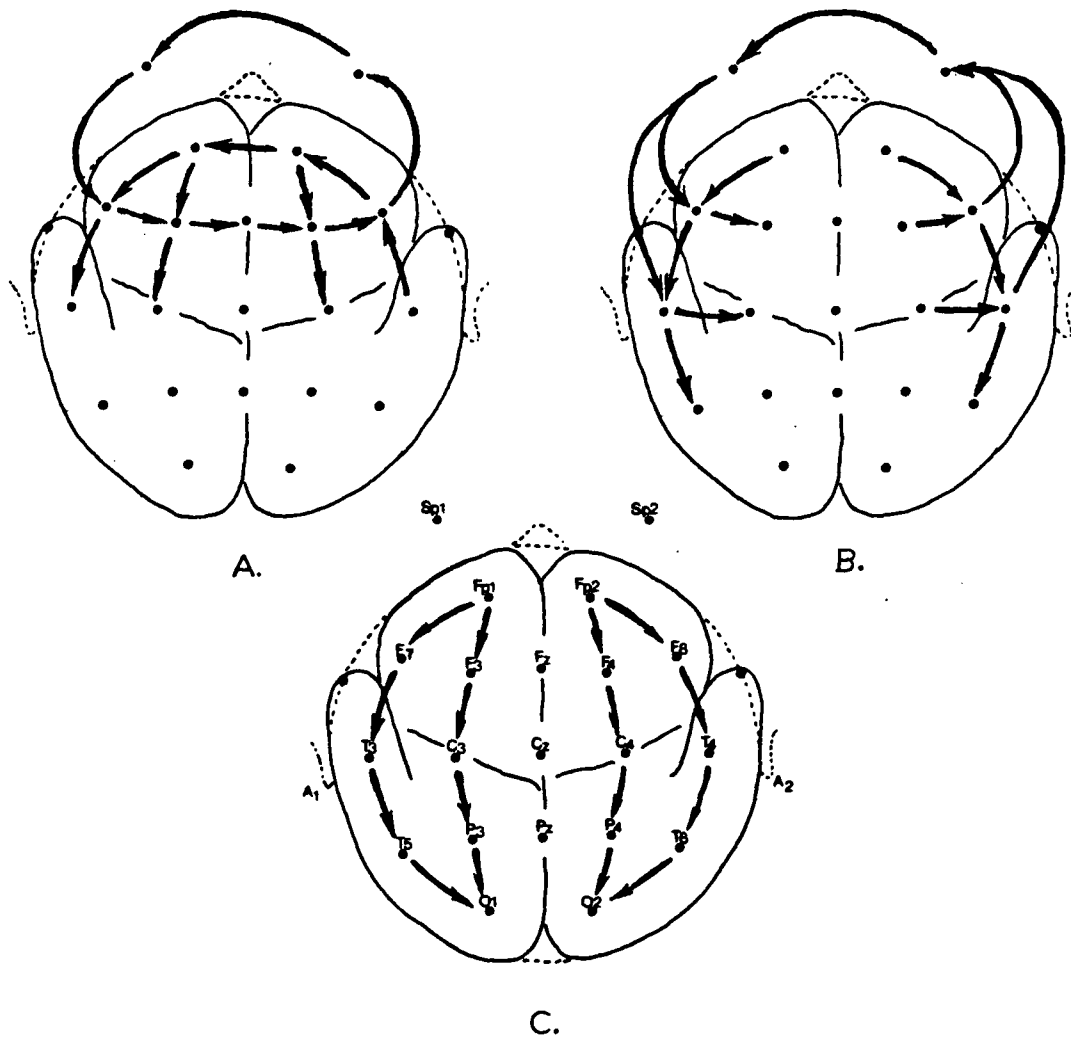
Figure 5 Typical Bipolar Recording Montages.

The EEG is influenced by several factors: age, mental state, region of brain, heredity, disease or drugs, technical and biological disturbances.[16] Traditionally, the EEG has been described in terms of characteristic rhythms (alpha, beta, delta, theta - figure 6), transients (spikes, sharp waves - figure 7), and artifactual content (figure 8). Scientists have been able to correlate certain brain abnormalities and states of conciousness with these signal characteristics. Various stages of sleep, for example, are defined partially by dominant EEG rhythms. It is possible in many cases to distinguish between normal and abnormal EEG. The exact physiological mechanisms which generate patterns, however, is not known.

A typical EEG recording session will last for half an hour. The environment is designed to minimize interference. As movement usually causes the greatest problems, the patient is asked to remain still for the entire period. The session may include several periods of eyes open and closed, hyperventilation, or photic stimulation. It may also be necessary to study subjects over prolonged periods, with such sessions lasting days or weeks. The patient has much more freedom to move about (thanks to the introduction of telemetry equipment), thus, EEG recorded during these sessions is corrupted to a large degree by artifact.
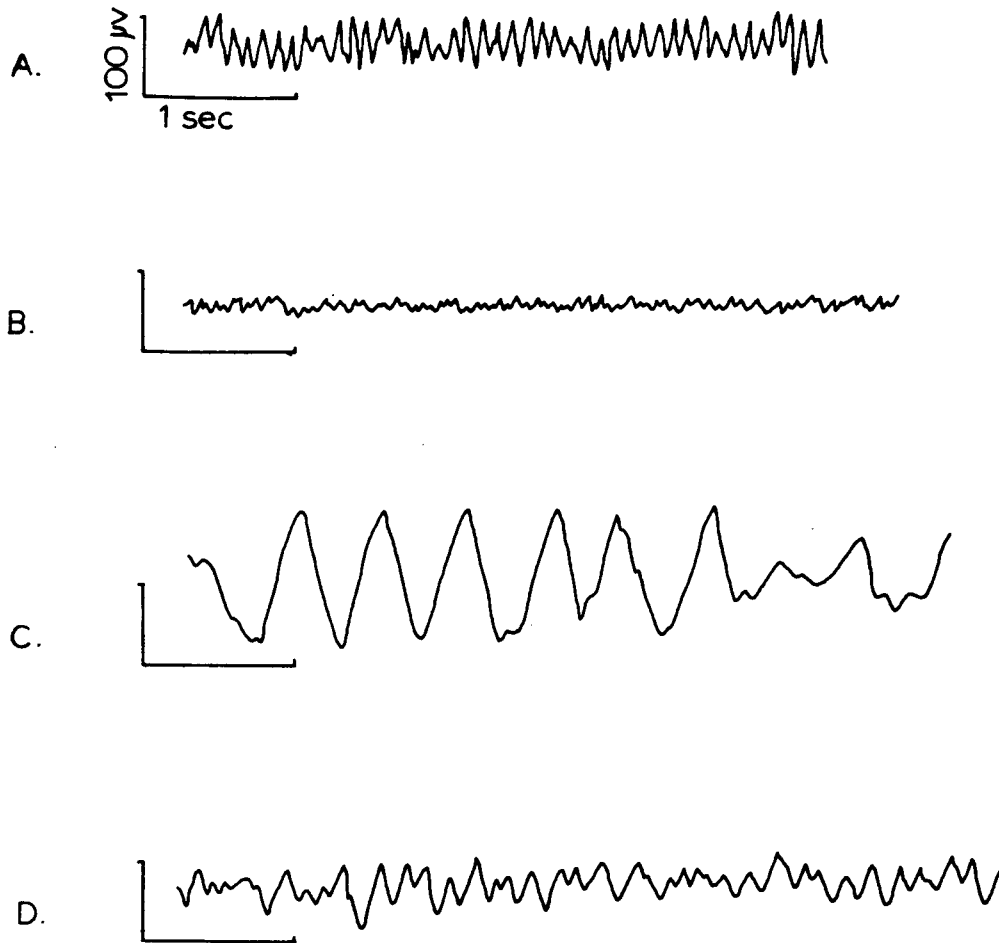
Figure 6 EEG rhythms; (a)alpha, (b)beta, (c)delta, (c)theta.
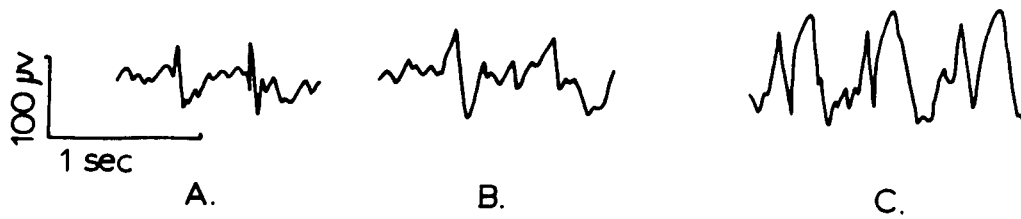
Figure 7 EEG transients (a)spikes, (b)sharp waves, (c)spike and wave.
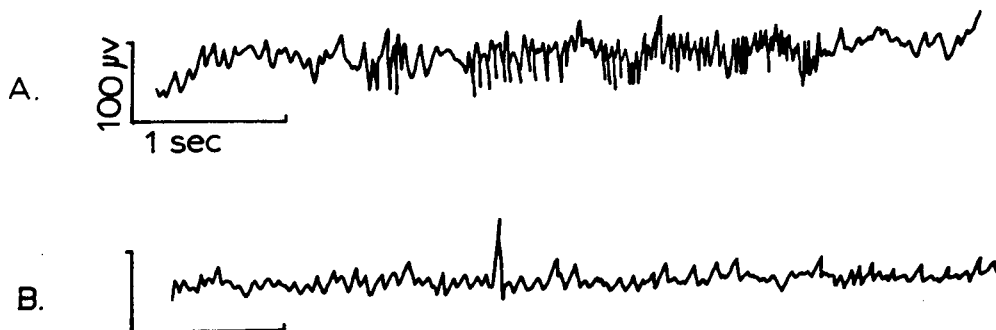
Figure 8 EEG artifact.

2.2 Epilepsy

Epilepsy first came to be known by its clinical manifestations. Muscular spasms, disorientation, loss of vision, aggressive or violent behavior are all possible signs. Only with the introduction of electroencephalography as a clinical science did epilepsy also begin to become characterized electrographically. Electrically, epilepsy is characterized by "synchronous discharges of large groups of neurons, often including the whole brain".[38]

There are many manifestations of seizure activity in the EEG including: desynchronization of EEG and decrease in amplitude; moderate or high amplitude rhythmic activity in the range of 1 to 30 hz, high amplitude EMG, or irregular paroxysmal activity. Petit mal seizures are identified by a feature known as spike and wave (figure 7c). In severe grand mal seizures EEG waveforms are characterized by high amplitude activity over the whole of the cortex. Seizure activity may be contained in one hemisphere of the brain - it may be in both. Some smaller seizures may exhibit no obvious change in the EEG at all. Another type of seizure (subclinical or electrographic) is characterized solely by EEG manifestation.

There is also evidence of intermittent, non-periodic, between seizure (interictal) activity. This takes the form of sharp transients known as spikes or sharp waves (SSW). The morphology of interictal activity is used as a diagnostic tool,

particularly for locating epileptic focii. Unfortunately, there is no simple definition of SSW's. Neurologists often differ as to whether or not an individual waveform is an SSW[2] and decisions are based more on experience and intuition than the application of fixed rules.

Some workers[6,19] have attempted to quantify SSW according to standard parameters; amplitude, slope, and duration. Others[9,21] have examined shape characteristics such as asymmetry between rising and falling phases of the SSW. Duration (spikes - 80 milliseconds, sharp waves - 200 milliseconds) is an important distinguishing feature, however, sharpness is the principle one. The sharpness necessary to define SSW depends on the background activity, although some workers[20] have attempted to define it in absolute terms.

2.3 Automation Of EEG Evaluation

Electroencephalography was slower to take advantage of automated techniques than other clinical sciences but in the last decade and a half there has been a large increase of work in this area. No doubt, the availability of integrated circuits and minicomputers was the key factor spurring on the automation of clinical electroencephalography. The goal of fully automating routine clinical EEG examinations has, however, not been realized. Two factors are important: lack of knowledge of EEG and its origins and the lack of necessary computing power.

The impact of microprocessors and VLSI technology on the latter problem remains to be seen.

Automated EEG analysis has focused on several areas:[8] (1) Studying the range of EEG variation in terms of standard parameters and development of standardized data bases, (2) Frequency analysis of background activity, (3) Detection of clinically significant transient activity, (4) Development of simple, meaningful displays, and (5) Classification of standard patterns and feature extraction.

Computer analysis of EEG offers the potential for aid in (1) freeing the specialist from tedious, time consuming tasks of classification and (2) gathering information which was hitherto unavailable. The latter may involve (a) applying standard analysis to very long recordings to increase the _amount_ of information[12] or (b) defining new features and parameters invisible to the human eye to increase the _types_ of information available.

2.4 Automatic Detection Of SSW

2.4.1 Non-parametric Methods

Attention has focused on the task of developing automated methods for detecting epileptiform spikes and sharp waves (SSW). Claims have been made of limited success in accurately locating regions where epileptic activity originates[14 24], however,

much work remains to be done.

The most popular parameter used in existing SSW detection schemes is the sharpness of a waveform. There is some support for the hypothesis that epileptiform and non-epileptiform waves form two separate statistical populations in terms of their sharpness[25 36] (see figure 9). Several methods using some form of sharpness criterion (first or second derivative) are described in the literature. Earlier systems[5 34 37] employed operational amplifier differentiators, timers, and other specialized analog circuitry. One problem with the analog methods is the inability to reject high frequency artifact. Filters which adequately attenuate muscle activity also distort the spike waveforms. Current approaches involve digital bandpass filters. These techniques[22 29 36] don't eliminate the problem of muscle artifact but records can be further processed using non-linear operations.

Gotman and Gloor[11] have had considerable success with a heuristic method which examines several parameters, including sharpness of the wave. The EEG signal is decomposed into sequences or half waves. These are characterized by a relative amplitude and a duration which form a two dimensional decision space for acceptance of the half waves as being potential components of an epileptic transient. After treating half waves separately, full waves are examined according to amplitude and sharpness. Tests are performed to reject major sources of artifact.

Template matching schemes have been used with limited success. Pola and Romagnoli[31] reported using a template matching method for spike detection in the differentiated signal of stereoelectroencephalograms (SEEG). The authors state that "the accuracy of the method ranges between 67% and 95%. Such a range depends exclusively on morphology of the examined spikes." The problem is that morphology is widely variant and it is questionable if a system which uses a small enough set of templates to be practical can be implemented. Salzberg et al[33] described a more sophistocated, adaptive approach which involves training the system on EEG spikes. Depth electrodes were used to detect the presence of spikes. The EEG was summed coherently each time there was a spike in a depth electrode. The spectrum of this coherent sum was divided by the noise spectrum (background EEG) and then, using the inverse Fourier Transform, a template was obtained which could then be convolved with EEG for spike detection. This method was applied to a very limited number of spikes, with discouraging results.

All these methods are similar in that they assume a model of the ideal SSW which can be represented by a fixed set of parameters. The signal is then processed to find sections whose parametric measures are within an acceptable tolerance.
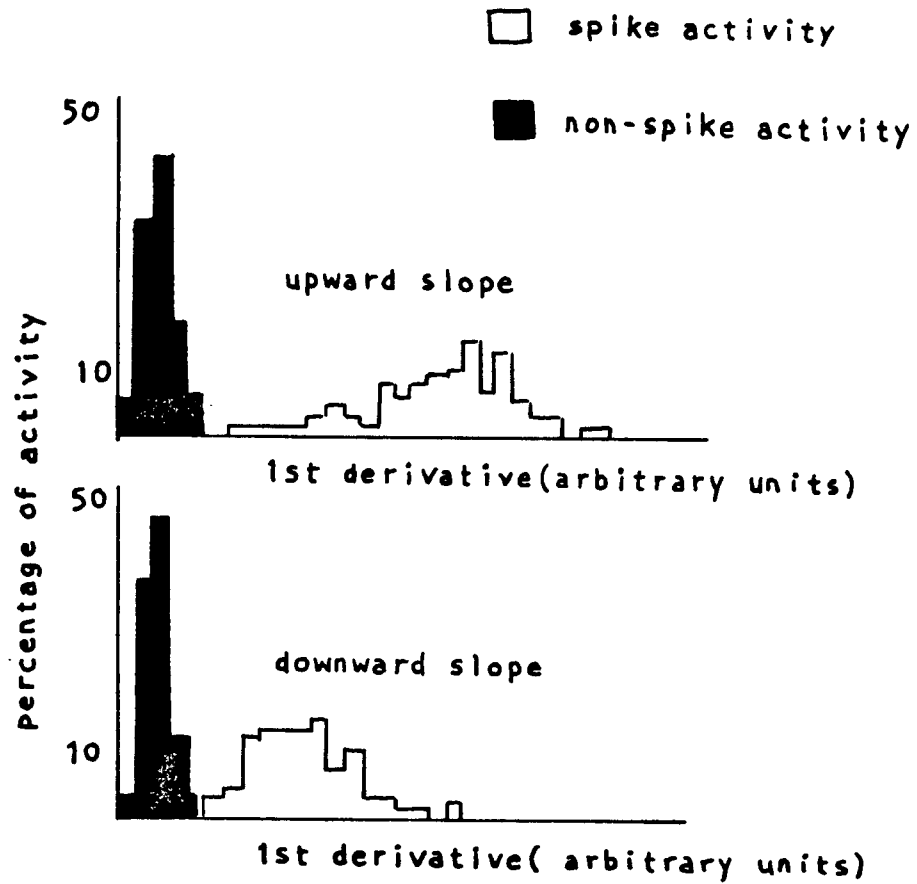
Figure 9 Distributions of Maximum First Derivatives of EEG. SSW and background appear to form separate populations in terms of waveform sharpness.

2.4.2 Parametric Methods Of SSW Detection

Some investigators have attempted to instead develop a linear, parametric model of the background or normal EEG activity. In processing the signal, they look for sections which do not have the same background statistics. These sections are candidates for epileptic transients.

We assume that EEG is stationary over, at least, some small period of time (ie. 5 seconds). We assume further that the signal, $y(n)$, is the output of a linear system, $h(n)$, with input $g(n)$, a white Gaussian sequence.

Then,
$$y(n) = -\sum_{k=1,p} a(k) \cdot y(n-k) + Ko \cdot \sum_{i=0,q} b(i) \cdot g(n-i) \qquad \ldots 2.1$$

or, if $H(z)$ is the transfer function of the system;
$$H(z) = Y(z) / G(z) \qquad \ldots 2.2$$

$$= [Ko \cdot (1 + \sum_{i=1,q} b(i) \cdot z^{-i})] / (1 + \sum_{k=1,p} a(k) \cdot z^{-k}) \qquad \ldots 2.3$$

Normally, an all-pole or autoregressive model is used. The coefficients $b(i) = 0$ for $i > 0$. The gain factor, Ko, is an arbitrary constant which can be set to 1.

$$y(n) = -\sum_{k=1,p} a(k) \cdot y(n-k) + g(n) \qquad \ldots 2.4$$

$$H(z) = 1 \,/\, (1 + \sum_{k=1,p} a(k) \cdot z^{-k}) = 1 \,/\, A(z) \qquad \ldots 2.5$$

If the input, $g(n)$, is unknown and the signal is predicted from past values, then we have the predicted signal, $y'(n)$, such that;

$$y'(n) = -\sum_{k=1,p} a(k) \cdot y(n-k) \qquad \ldots 2.6$$

Thus, $\quad g(n) = y(n) - y'(n) = e(n) \qquad \ldots 2.7$

In determining the coefficients, $a(k)$, we want to minimize the prediction error, $g(n)=e(n)$. Using least squares minimization, we obtain a matrix equation which can be solved to get the coefficients, $a(k)$.

$$
\begin{bmatrix}
R(0) & R(1) & R(2) & \ldots R(p-1) \\
R(1) & R(2) & R(3) & \ldots R(p-2) \\
R(2) & R(3) & R(4) & \ldots R(p-3) \\
\cdot & \cdot & \cdot & \cdot \\
\cdot & \cdot & \cdot & \cdot \\
\cdot & \cdot & \cdot & \cdot \\
R(p-1) & & & \ldots R(0)
\end{bmatrix}
\begin{bmatrix}
a(1) \\
a(2) \\
a(3) \\
\cdot \\
\cdot \\
\cdot \\
a(p)
\end{bmatrix}
= -
\begin{bmatrix}
R(1) \\
R(2) \\
R(3) \\
\cdot \\
\cdot \\
\cdot \\
R(p)
\end{bmatrix}
$$

$$\ldots 2.8$$

A method by Durbin[26] involves a simple recursive procedure for solving equation 2.8.

We now have a model of the stationary EEG signal whose output is the product of passing white, Gaussian noise through a linear system, $H=1/A$. In other words, the EEG is modelled as

colored Gaussian noise. It is clear from this discussion that A(z) is a whitening filter. In theory, if EEG is passed through it we obtain a random, uncorrelated sequence, e(n), whose spectrum is flat.

If there is a transient (ie. SSW) in the EEG which is statistically insignificant in the calculation of the a(k)'s, then the output of the whitening (or inverse) filter will have a higher amplitude since it is the prediction error. As such, the inverse filtering operation is used as a detector of epileptiform transients.

The parametric approach has been used by a number of workers. All use the whitening filter, but once e(n) is obtained, the similarity in methods disappears. Some use a simple amplitude threshold on e(n) for transient detection while others (Zetterberg) used $e(n)^2$. Lopez da Silva[23] sum $e(n)^2$ over a short interval before testing against a threshold. Others have applied a second differential operator to e(n) and set a threshold level for that.[3] Still others suggest combining the whitening filter with the matched filter.[1,30]

Advantages to using the parametric approach include an apparent ability to detect SSW so obscured by background noise that they are missed by the human eye. Another advantage is that, as a byproduct of the method, we get a reliable spectral estimate of the background activity. The Durbin method even makes it possible to specify the degree of spectral resolution of the estimate, so that only significant resonances are

resolved.

There are problems with the parametric approach. The analysis assumes stationarity of the signal. Since signal statistics can change abruptly, however, the reliability of the filter may be questioned. Bodenstein[4] and Michael[28] have attempted to tackle this problem by first segmenting the data according to statistical requirements. There may also be problems when the training segment contains artifact or a number of SSW. This will bias the spectral estimation and so degrade the effectiveness of the detection. The cost in computation time of the parametric method might be considered problematic for certain applications (especially for real-time detection). Finally, it should be noted that the parametric method is not an SSW detection method: it is a transient detection method. Only a small number of EEG transients are SSW, thus it is still necessary to distinguish the SSW from the other classes of short transients.

III. DETECTION OF EPILEPTIFORM TRANSIENTS: THEORETICAL CONSIDERATIONS

We know of only one comparative study[3] of SSW detection methods and it is strictly empirical in approach. Using statistical detection theory, we will introduce the notion of error probability as a performance criterion for SSW detection. We will describe a computer model which computes a theoretical performance level for SSW detectors using signal-to-noise ratio (SNR). This model is used to analyse a parametric method and the simple slope detection scheme (bandpass) we have implemented in our EEG monitor.

3.1 <u>Assumptions In Characterizing Background EEG And SSW</u>

In the SSW detection problem we will assume that EEG, $v(t)$, is a superposition of SSW, $s(t)$, and noise, $n(t)$ (see figure 10). The noise is random, but assumed to be colored, Gaussian, and stationary. The assumptions of Gaussianity and stationarity have been shown, for short segments of 5 seconds or less, to have some experimental justification.[27] We will assume that the presence of $s(t)$ does not affect the statistical properties of $v(t)$. Thus, statistics of $n(t)$ can be obtained directly from $v(t)$. What is known about spikes is vague. There is considerable variation in amplitude, duration, and waveshape. Sharp waves, which are quite different from spikes, can also occur. Later, we will describe SSW in statistical terms, ie. power spectrum only. Here too, however, variations permit only a general description.

Figure 10 Model for EEG Signal, $v(t)$.
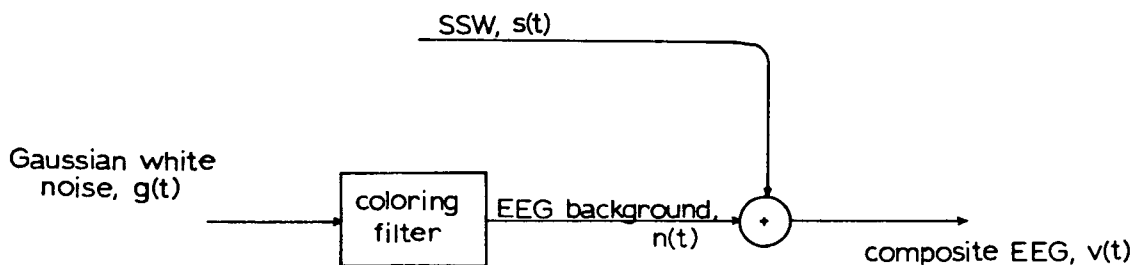
<u>Figure 10</u> Model for EEG Signal, $v(t)$.

3.2 Error Probability In Binary Detection Systems

Detection of epileptiform transients falls into the most elementary class of detection systems; those which ask if a signal is present or not. In such systems, a useful performance criterion is detection probability and a basic measure of performance is probability of error, Pe. There are two types of error probability in this system; (1) that an SSW is present and the system misses it (false rest probability = Pfr) and (2) that there is noise alone but the system falsely detects an SSW (false alarm probability = Pfa).

In an N-dimensional decision space we have N parameters, $v_1 v_2 ... v_n$, that are outputs of the system (figure 11). Then

$$Pfr = \iint ... \int_{Rn} dv_1 dv_2 ... dv_n \ ps(v_1 v_2 ... v_n) \qquad ...3.1$$

$$Pfa = \iint ... \int_{Rs} dv_1 dv_2 ... dv_n \ pn(v_1 v_2 ... v_n) \qquad ...3.2$$

where $ps(v_1 v_2 ... v_n)$ is the joint probability function for $v_1 v_2 ... v_n$ if an SSW occurs and $pn(v_1 v_2 ... v_n)$ if noise alone occurs. Rs is the region of acceptance for SSW in the N-dimensional space, while Rn is the region for noise alone. Theoretically, if the above probability density functions are known, we know the probability of detection error, Pe, in the system.

$$Pe = Pfr + Pfa \qquad\qquad ...3.3$$

Our goal is to reduce Pe. We can reduce the region Rn to

minimize Pfr, but that increases Pfa: reducing Rs will increase Pfr. False rest error can only be decreased at the cost of increased false alarm error and vice versa. The combination of these errors, Pe, should be minimized subject to one of the criteria defined below.

1) The ideal observer criterion - overall error probability is minimized.

2) The minimum average loss criterion - a loss factor is assigned to each type of error, Pfr and Pfa, and the combined loss is minimized.

3) The Neyman-Pearson criterion - false rest probability is minimized for some fixed false alarm probability.
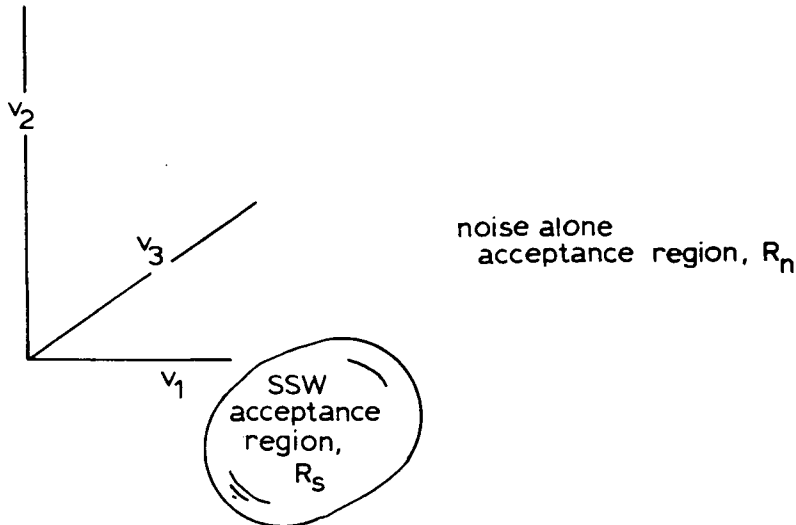
Figure 11 A 3-Dimensional Decision Space.

3.3 Model For Evaluation Of Detectors

In linear systems, error probability is a monotonically decreasing function of signal-to-noise ratio at the output of the system (SNRo). Therefore, SNRo is a good measure of system performance, which is fortunate because it is easy to calculate.

To better understand the usefulness of particular filters, F_k , we have created a computer model that generates simulated EEG spectra and calculates theoretical input and output SNR for each filter.

$$\Lambda_k = SNRo/SNRi \qquad \qquad ...3.4$$

The quantity, Λ_k, of equation 3.4 is an improvement ratio in SNR from input to output. It provides a good comparative measure for filters. We would hope that Λ_k be at least 1.0 for all possible EEG spectra and considerably greater than 1.0 for a large class of them.

Calculation of Λ_k for a particular filter is quite straight forward. Output power spectral density (psd), Po(f), from a linear system is simply;

$$Po(f) = |F_k(f)|^2 \cdot Pi(f) \qquad \qquad ...3.5$$

where $F_k(f)$ is the filter transfer function and Pi(f) is the input power spectral density. Making use of the model of EEG background as filtered white noise we have the situation as shown in figure 12. The psd of EEG background, N(f), is

$|H(f)|^2 \cdot Gn(f)$, where $Gn(f)$ is the psd of white noise and $H(f)$ is the system function which colors the noise. Thus,

$$SNRi = \int_{-\infty}^{\infty} Q(f)df \Big/ \int_{-\infty}^{\infty} N(f)df \qquad \ldots 3.6$$

$$SNRo = \int_{-\infty}^{\infty} |F_k(f)|^2 \cdot Q(f)df \Big/ \int_{-\infty}^{\infty} |F_k(f)|^2 \cdot N(f)df \qquad \ldots 3.7$$

where $Q(f)$ is the psd of the SSW whose Fourier Transform is $S(f)$. Using the relations in the above equations, Λ_k can be calculated for each filter.
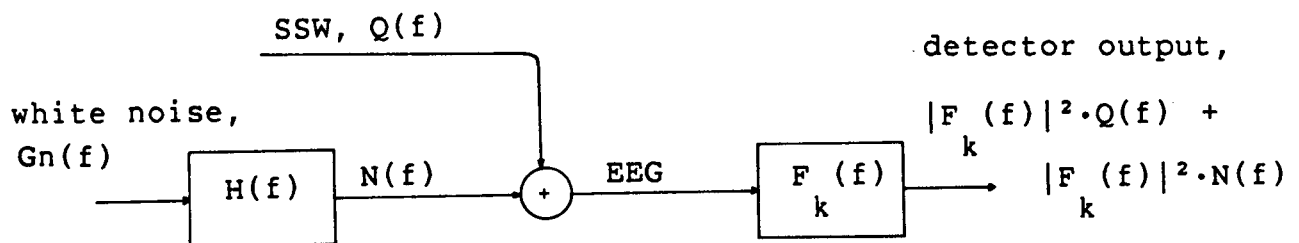
Figure 12 Change in Power Spectral Densities due to Linear Filter.
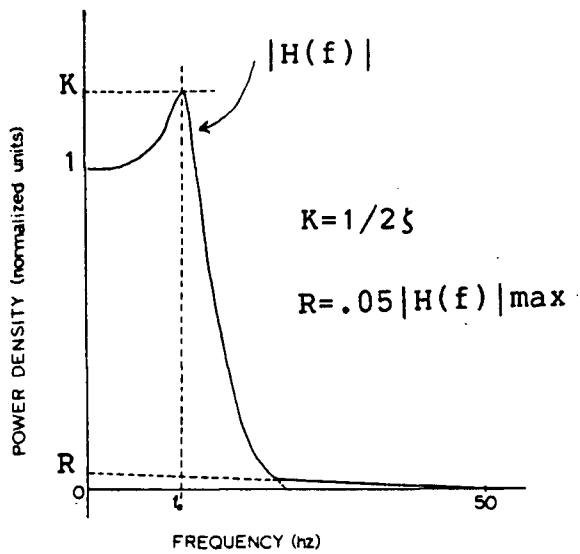
Figure 13 Spectral Model of EEG Background. EEG spectrum is modelled using a second order function of natural frequency f_o and damping factor ζ. A linear function takes over for higher frequencies.
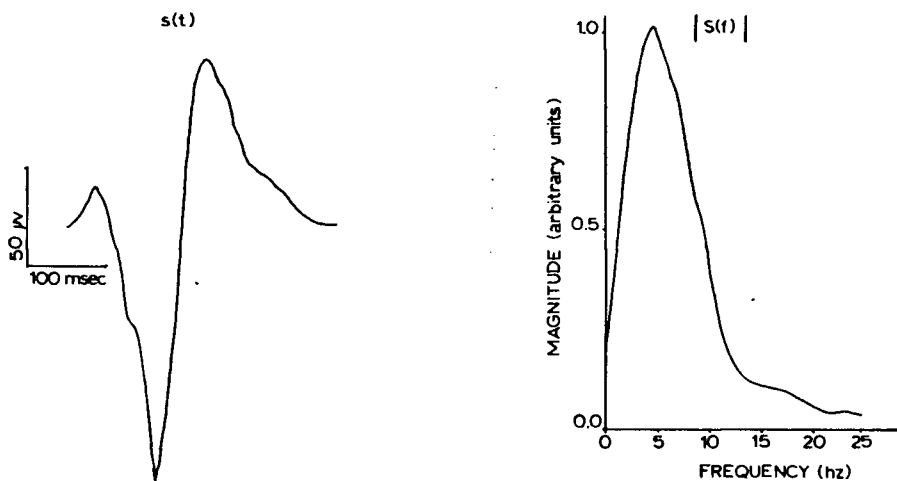
Figure 14 Spike Model and its Frequency Representation.

To model the EEG spectrum, H(f), we used the scheme shown in figure 13. The transfer function, H(f), was generated using a second order function of natural frequency, fo, and damping factor, ζ. In order to more realistically represent the high frequency content, we used a second, linear function beginning at .05 of the maximum height of the second order function and declining to 0 at 50 hz. This is necessary when considering the inverse spectral filters, otherwise high frequencies are unrealistically magnified in the model. The psd for SSW was obtained by taking actual SSW (figure 14) from EEG records and performing FFT's to get S(f). The integrals of equations 3.6 and 3.7 were solved numerically on a general purpose computer.

Initially we compared three filtering methods: (1) a simple bandpass, $F_1 = 2j \cdot \{\sin(2\pi f) + \sin(4\pi f)\}$, (2) the inverse spectral filter, $F_2 = 1/H(f)$, and (3) the unrealizable, optimal matched filter, $F_3 = \{S^*(f) \cdot \exp(2j\pi f)\} / \{ H(f) \}$ (unrealizable because in practice we don't know S(f)).

3.4 Results Using Simulated Spectra

Results are shown in figure 15. The first observation of interest is the sub-optimality of filters F_1 and F_2 compared with the matched filter, F_3. Λ_3 never falls below 1.0 and only approaches it in a very small region. Where Λ_3 approaches 1.0 is understandable because it is for H(f) which are similar in form to S(f). If signal and noise have identical spectra, the matched filter will pass both unattenuated and the SNR gain, Λ_3,

will be 1.0.

Another interesting result is that, although the actual values of Λ_2 and Λ_3 are much different, the contour plots are similar in shape. F_2 is merely a whitening filter and the first stage in the implementation of F_3. Since the SNR gain in detecting a signal in white noise with a matched filter is approximately constant[32], Λ_2 and Λ_3 should also differ by a constant. The constant factor is Bn/Bs, where Bs is the spike bandwidth and Bn is the bandwidth of the whitened noise. In fact, this will not be exactly constant since the whitening process of F_2 alters the spectrum of s(t).

Theoretically, if the SSW spectrum reaches into any range of frequencies where there is no noise power, the measure, Λ_2, goes to infinity (flawless detection). This is because the inverse filter will infinitely boost signal power in the bands where there is no noise. In practice, this doesn't happen. The results here demonstrate what happens for the non-ideal cases.
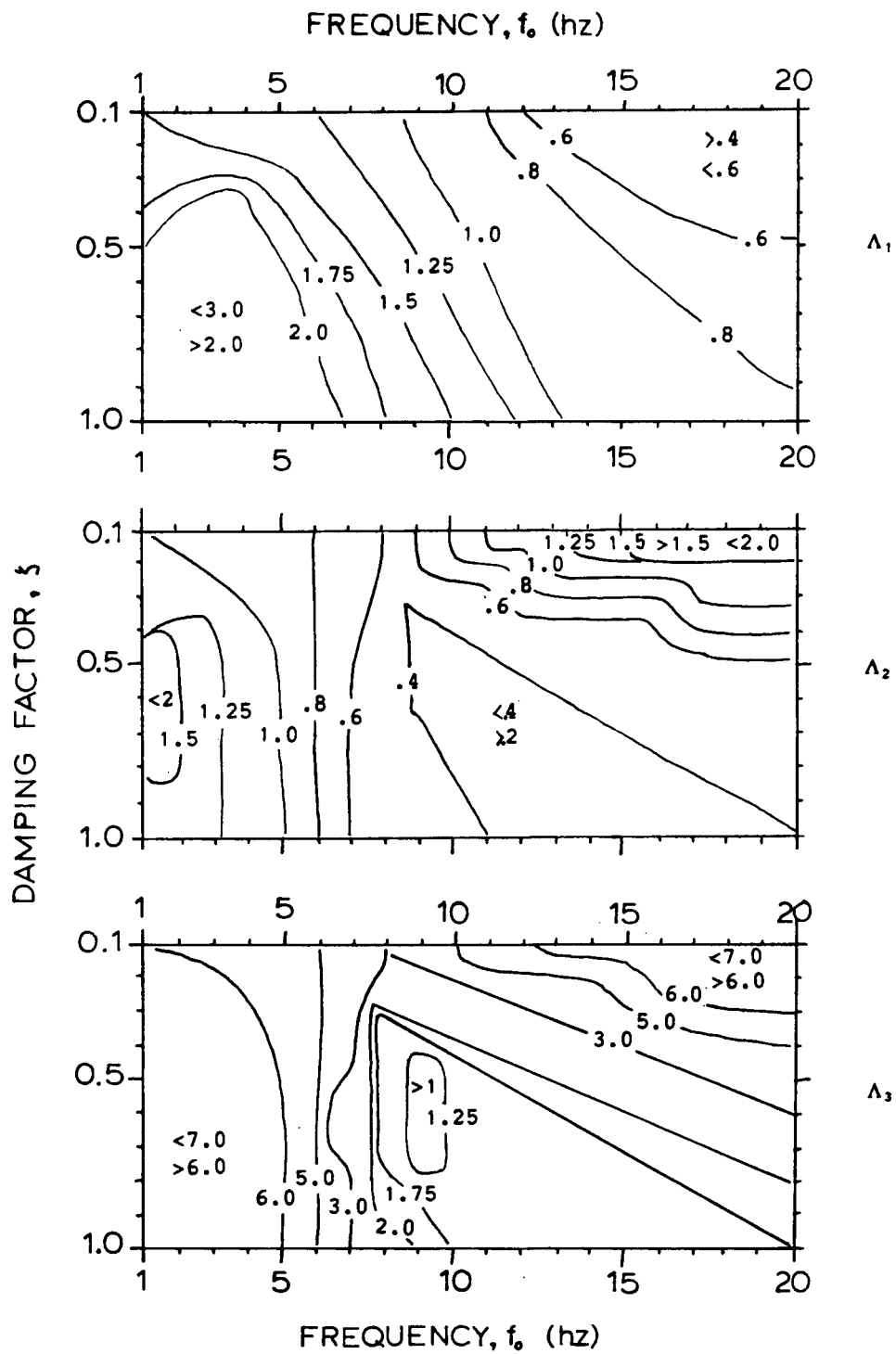
Figure 15 SNR Gain: (a) Λ_1, (b) Λ_2, and (c) Λ_3.

When there is a coincidence of SSW spectra and noise spectra the results can be devastating for output SSW power (figure 16). The inverse filter suppresses noise but it is totally indiscriminate in dealing with SSW power because it assumes no prior knowledge of it. Even when there is considerable separation of the SSW and noise spectra, the result may not be good. In the case shown in figure 17 the inverse filter will boost power by a factor of R. Because this is done across the whole spectrum, however, noise power is also increased by a factor of Bn/Bc, where Bc is the bandlimit of the colored noise. The SNR improvement from input to output will be R·(Bc/Bn) which could be less than 1 if the ratio Bc/Bn is too small. If we study the contours, Λ_2, in figure 15b we see that the best results are obtained at very low frequencies or at higher frequencies if the noise power is concentrated in a narrow band. When the noise spectrum is spread out, the SSW power is severely reduced by the inverse filter.
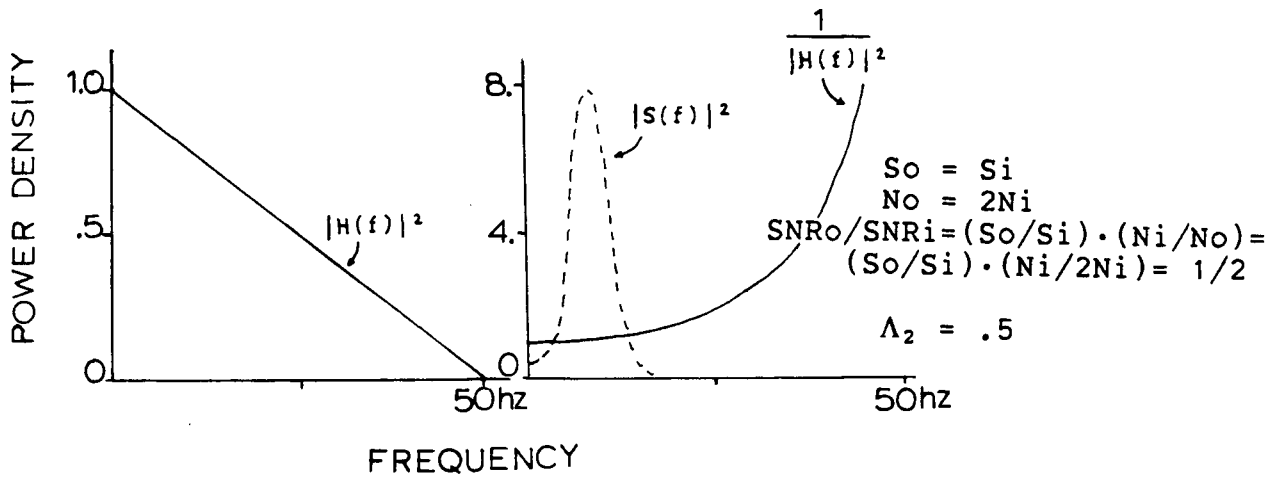
Figure 16 Coincidence of SSW and Noise Spectra. For this kind of EEG spectrum (H(f)) the inverse filter (1/|H(f)|²) favors frequencies outside the range where most SSW power is located.
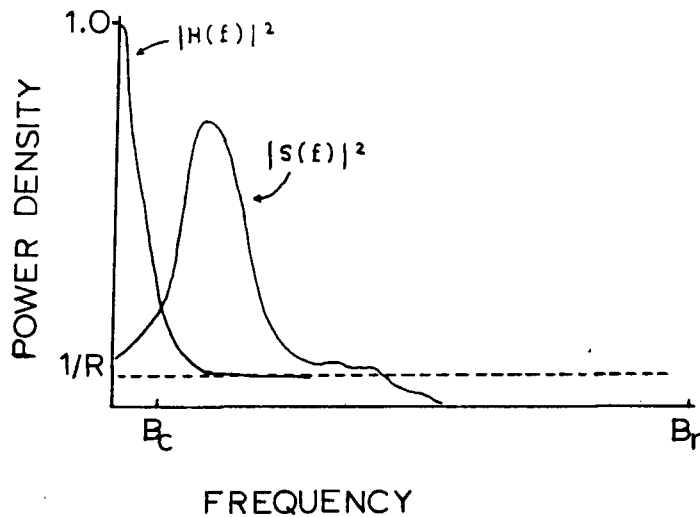
Figure 17 Separation of SSW and Noise Spectra. Since $\Lambda_2 = R\cdot(Bc/Bn)$, if $R = 10$ and $Bc = .1\cdot Bn$, then Λ_2 is only 1.

One parametric method usually follows the inverse filter, F_2, with a squaring and summing operation. We have already seen the effect of the inverse filtering. To calculate the contribution of the squaring and summing (autocorrelation) we make use of the relation[32];

$$\Lambda p = \Lambda_3 \cdot \{ 1/ (1+4Bn \cdot T)\} \qquad \ldots 3.8$$

where Λp is the SNR improvement for the parametric method (including autocorrelation), T is the integration time = (N-1)$\cdot$to (to = sampling period), and T>>1/Bn. Since Λ_3 is the improvement factor for a matched filter, it can be expressed as $\Lambda_2 \cdot$(Bn/Bs). The effect of the autocorrelation operation itself, Λa, is;

$$\Lambda a = \Lambda p / \Lambda_2 = (Bn/Bs)/(1+4Bn \cdot T) \cong 1 / 4Bs \cdot T \ldots 3.9$$

Lopez da Silva[23] reports using a value of 25 milliseconds for T. Substituting this into equation 3.9, we must have that Bs is less than 10 hz in order that Λa be greater than 1. Thus, the detectability of a signal in white noise by this method is dependent on the signal's bandwidth. Values for Λp can be obtained directly from the contours of Λ_3. Since $\Lambda p = .2\Lambda_3$, the 1.0 contour of Λp is equivalent to the 5.0 contour of Λ_3. Comparing this to figure 15b, we see that the summing and squaring operation offers some small improvement in detection capability over simply applying the inverse filter (ie. $\Lambda a > 1$). It should be noted, though, that we have been lenient in allowing T = 25 milliseconds and so violating the condition that T>>1/Bn. In reality, T should be made much larger, thus

reducing the factor, 1/(1+4Bn·T), in equation 3.9.

Figure 18 shows a comparison of the SNR improvement ratios for the inverse filter and the simple bandpass detector. The bandpass, F_1, works best at lower frequencies and when the EEG spectra is more distributed. If most of the noise background is concentrated in a resonant peak, F_1 can even worsen the situation unless the resonant frequency is low. In general, however, it compares very favorably to the inverse filtering method. The only advantage of the inverse filter over the bandpass method is for a few spectra with strong resonant peaks at higher frequencies.
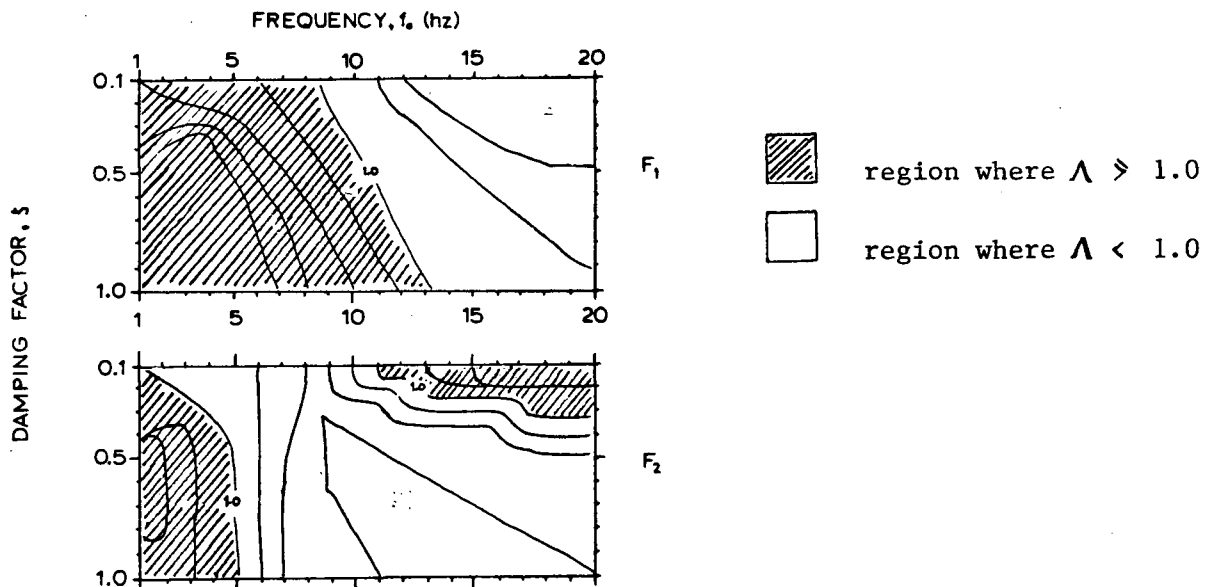
Figure 18 Types of H(f) for which SNR Gain is > 1.0.

A.

B.

C.

0.0   1.25   2.5   3.75   TIME (seconds)
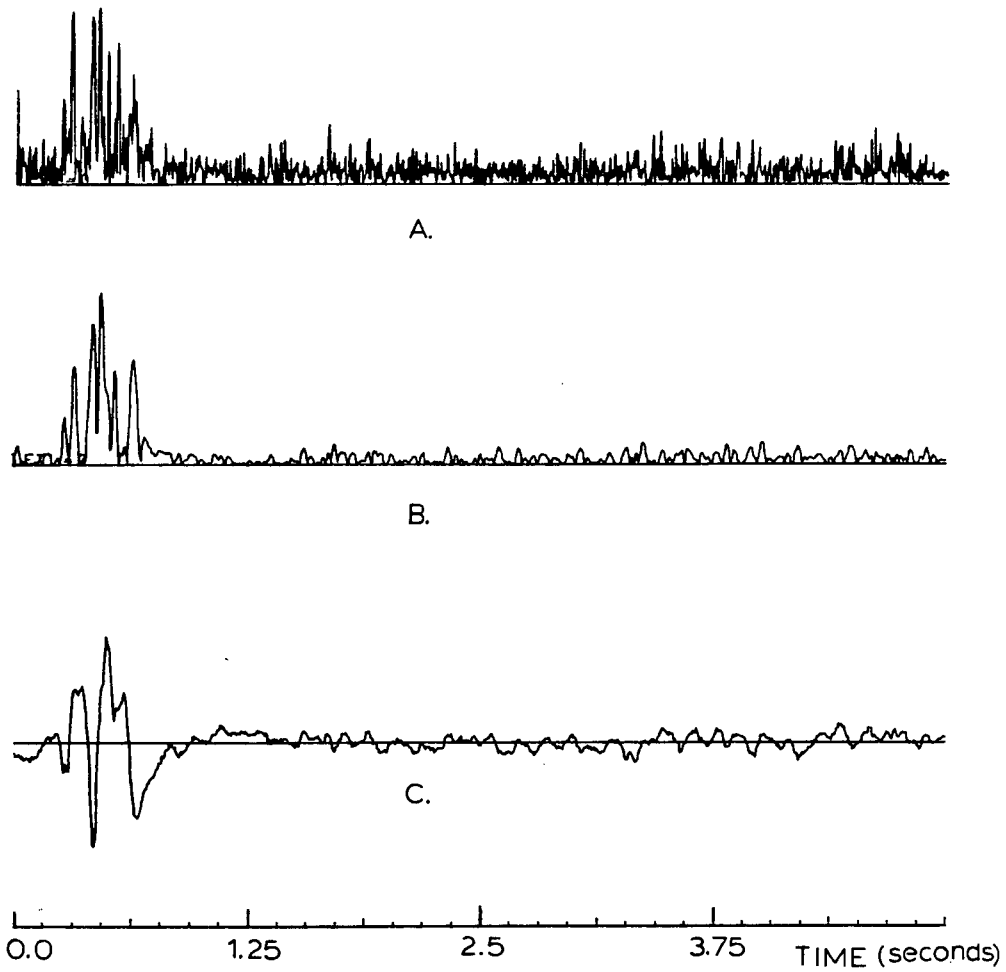
Figure 19 Results of SSW detection. (a) The inverse filter and
(b) a bandpass detector.

In theory, the SNR gain from input to output of the inverse filter could be infinite. In practice, we have found (figure 19) the inverse filter to give results no better than a simple bandpass detector. This model shows, theoretically, that this can be expected for many types of EEG background. Intuitively, the bandpass filter, F_1, seemed like a good choice as a detector since SSW are often characterized by their steep slopes. In addition, it is almost trivial to implement when compared to the complexity of the inverse filter. We have seen that it is a good detector of SSW in low frequency activity such as delta or theta. It has problems with higher frequency activity such as alpha or muscle (figure 20) but it would be difficult to find any single operator that functions well as a detector of SSW in all kinds of EEG background. Our approach has been to use this operator, which functions well as a detector of SSW in a broad class of EEG, and to develop separate strategies for the cases where it is poor (muscle and alpha activity).
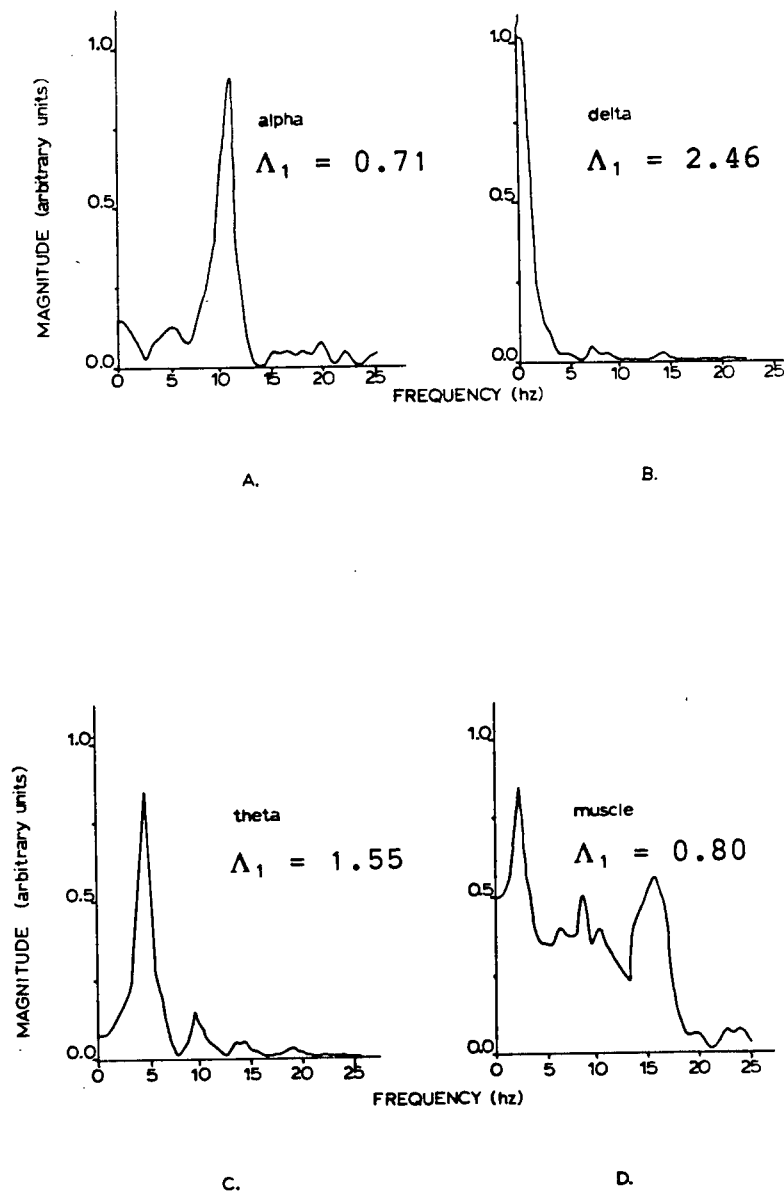
Figure 20 Response of F_1 to Typical EEG. SNR Improvement ratio, Λ_1, was calculated using background spectral model for (a) alpha, (b) delta, (c) theta, and (d) muscle activity.

IV. A SIMPLE DETECTOR OF SSW

Detecting SSW in EEG with success has been reported by many workers. Most of these systems process the EEG off-line and on sections of data preselected to contain a minimum amount of artifact. We are interested in real-time detection for long term recording sessions using a simple microprocessor based system.

Our strategy for detection of SSW is to select candidate transients on a first pass with a low-level operator. The more complex and time consuming processing is then applied only to the reduced data. Specifically we will describe the design of:
   (1) the low-level operator (a bandpass)
   (2) shape tests
      a) duration
      b) form factor or 'wiggliness'
      c) triangularity
   (3) artifact rejection filters
      a) muscle
      b) alpha rhythm and spindles
We will also describe a method for detecting phase reversals when bipolar montages are used.

4.1 Lowpass Differentiator (Bandpass)

A differentiator highlights the sharp positive and negative slopes of a waveform. Since waveform sharpness is the main distinguishing feature of SSW, the differentiator is an obvious choice as an SSW detector. High frequency artifact, such as muscle activity, greatly affects the output of a pure differentiator. For this reason, differentiators which include a lowpass characteristic are desireable.

Ninomiya and Matsubara[29] used a linear regression operator for differentiation (equation 4.1).

$$b(k) = \sum_{n=-M}^{M} n \cdot x(n+k) \ / \ \sum_{n=-M}^{M} n^2 \qquad \ldots 4.1$$

The value b(k) is calculated for each sample time and represents an approximate differentiation of the signal. This is a linear transform with Z-transform, $F_4(z)$, as shown in equation 4.2.

$$F_4(Z) = Ko \cdot \sum_{n=-M}^{M} \{n \cdot Z^n\} \qquad \ldots 4.2$$

where $Ko = 1 \ / \ \sum n^2$

This is an easy operator to implement depending on the value of M chosen. It is particularly well suited to a recursive calculation of values.

An interesting paper by Usui and Amidror[35] compares a large number of digital lowpass differentiators. One of the simplest, and the one we chose for our low-level operator, has the following Z-transform.

$$F_1(z) = [\sum_{n=1}^{M} \{ z^{+n} - z^{-n} \}] / K_1 \qquad \ldots 4.3$$

$$\text{or} \quad b(k) = [\sum_{n=1}^{M} \{ x(n) - x(-n) \}] / K_1 \qquad \ldots 4.4$$

This is similar to equation 4.2 except for the weighting factor of each term in n. We see from the magnitude responses of the two operators, that they are quite similar (figure 21). F_1 is slightly broader in the main lobe but has a lower side lobe. F_1 also lends itself to recursive computation.

$$K_1 \cdot b(k) = K_1 \cdot b(k-1) + [x(k-M-1) + x(k+M)] - [x(k) + x(k+1)]$$

$$\ldots 4.5$$

This calculation is considerably simpler than for F_4, particularly when M is not a convenient number.
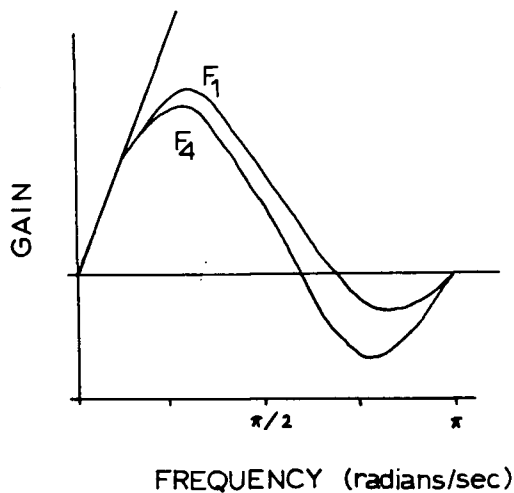
Figure 21 Frequency Response of lowpass differentiators.

4.2 Threshold Settings

We must put some threshold on the output of the bandpass filter in order to detect candidate SSW. The human eye does a considerable amount of processing to set a threshold. In addition to considering background level, the type of background is also important; (1)Amplifier gains are adjusted so that characteristic rhythms have a particular look, (2)If background statistics change abruptly, the eye will separate the signal into sections and consider each individually, (3)Transients are visually filtered out before setting a level, (4)The eye takes in activity from other channels.

In automated systems it is very difficult to match the processing done by the trained eye. Since the human considers a more global picture (activity over time and in all channels) an automated system would require a powerful processor and a huge amount of memory. Setting an absolute level is the simplest possible approach. At least one objection to this, from the neurologist's point of view, is that SSW are defined in terms of the background activity. Also, setting absolute thresholds requires a calibration procedure and this can be difficult since the signal may change drastically from one calibration period to the next.

An adaptive procedure which sets threshold levels according to the background a few seconds before and after the point concerned would be preferable. We set a threshold on the

bandpass output by considering 5 seconds of past activity. We assume that the EEG (and thus the bandpass output also) can be modelled as the output of a linear system whose input is Gaussian white noise (see Chapter 3). Following from this model it is a relatively simple matter to set some threshold level which corresponds to a low probability of acceptance of a given bandpass output value. The threshold, Th', is calculated from the relation 4.6.

$$Th' = Th \cdot \sigma \qquad \qquad ...4.6$$

where Th is the appropriate value from the table of the Normal Probability Integral, σ is the standard deviation of the background activity, and assuming the bandpass output to have zero mean over the 5 seconds.

This is not a difficult computation if it doesn't have to be done too often. It is even easier if we take advantage of an interesting property of Gaussian distributions described below. The probability density function, $\Phi(x)$, of a Gaussian distribution, $N(0, \sigma^2)$, is given in equation 4.7.

$$\Phi(x) = (1/\sigma\sqrt{2\pi}) \cdot \exp(-x^2/2\sigma^2) \qquad ...4.7$$

thus,

$$E(x) = \int_{-\infty}^{\infty} x \cdot (1/\sigma\sqrt{2\pi}) \cdot \exp(-x^2/2\sigma^2) \, dx \qquad ...4.8$$

which is easily shown to be = 0. (p.139 in ref.15)

But now consider $|x|$ instead.

$$E(|x|) = 2 \int_{0}^{\infty} (1/\sigma\sqrt{2\pi}) \cdot \exp(-x^2/2\sigma^2) \, dx \qquad ...4.9$$

Since the pdf of x is symmetric about the y axis

$$E(|x|) = (-2\sigma/\sqrt{2\pi})\cdot\exp(-x^2/2)\Big|_0^\infty = 2\sigma/\sqrt{2\pi} \qquad \ldots 4.10$$

and so,

$$\sigma = (\sqrt{2\pi}/2)\cdot E(|x|) \qquad \ldots 4.11$$

Using this result, the calculation of σ in equation 4.11 is very simple. Rather than calculating σ using the relation that $\sigma^2 = E(x^2)-E(x)^2$, we have only to find the mean of the absolute values, which is considerably easier. This result depends on the assumption of a zero mean, which is reasonable since the threshold calculation is done for 5 seconds of data.

4.3 Waveform Sharpness

In reality we are more interested in a second differential measure, since it is the sharpness of the waveform which is considered. We can achieve a double differentiation with two passes of F_1 or F_4. We could also use a single pass operator such as in equation 4.12 below. It is obtained by a least squares error fitting of a curve $y = a \cdot x^2 + b \cdot x + c$ to a set of points.

$$a = \{N\cdot \sum_{n=-M}^{M} [n^2 \cdot x(n) - N_2 \cdot S]\} / \{N \cdot N_4 - N_2{}^2\} \quad \ldots 4.12$$

$$\text{where } N_i = \sum_{n=-M}^{M} n^i \quad , S = \sum_{n=-M}^{M} x(n) \quad \text{and } N = 2M+1$$

Alternatively, we can take the difference of slopes from rising and falling phases. This approach, which is the one we

implemented, is simple and has the advantage of allowing us to set a minimum slope threshold for rising and falling phases independently. A waveform with one steep rising phase but a gradual opposite phase would not be accepted. A double differentiator may end up passing it as a possible candidate because the two phases cannot be considered separately.

4.4 Waveshape Of SSW

The bandpass operator alone leads to an excess of false detections and so a second stage of filtering is required based on waveform parameters, duration, form factor, and triangularity.

4.4.1 Duration

Spikes are generally defined as having a duration of 80 milliseconds and sharp waves 200 milliseconds. Leaving aside disagreements over these figures, we must deal with the definition of duration itself. Considering figure 22, we would intuitively chose duration to be δ_1, but if we were looking for a definition that was simple to implement, such as distance between slope zero crossings, we would end up with δ_2.

Gotman and Gloor[11] describe a somewhat arbitrary method that appears to work well. They define a pseudo duration as shown in figure 23. This pseudo duration is obtained by finding the point on the half wave which corresponds to the signal value

at the half duration. A line is drawn from the apex of the wave
and where it crosses the base line defines the pseudo duration,
δ'. This method is quite simple.

Let us model a half wave by a rectangle and a hyperbola as
shown in figure 24 and consider the two cases, A and B, shown.
In A, as the area under the hyperbola goes to zero, the pseudo
duration goes to $\delta/2$. There is a direct dependence on the
length of the tail. Clearly for the case of B, pseudo duration
goes to infinity. Thus, in the limiting cases the Gotman-Gloor
method is not a good representation of duration.

As an alternative to this method, we have used an approach
which finds the pseudo duration, δ'', by matching the area of an
ideal triangular wave of amplitude, Vm, and width, δ'', to the
actual area of the half wave of amplitude, Vm, and width, δ.
Referring to figure 25, we can write the relation shown in
equation 4.13 to define pseudo duration.

$$\delta'' = 2A/Vm \qquad \ldots 4.13$$

In the limiting cases discussed above, when the area under the
hyperbola goes to zero (case A) the pseudo duration goes to
twice the width of the rectangular part. In contrast to the
Gotman-Gloor method, the length of the tail is important only
insofar as it contributes more area to the half wave. As the
half wave becomes rectangular in shape (case B) the pseudo
duration goes to 2δ. This is not ideal but considerably better
than the Gotman-Gloor method.
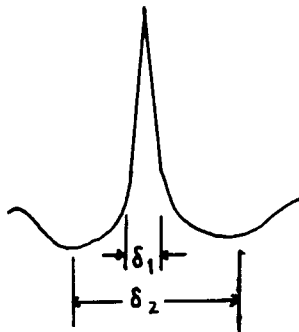
Figure 22 Definition of Spike Duration. An intuitive choice for duration measure is δ_1 but δ_2 is easier to compute.
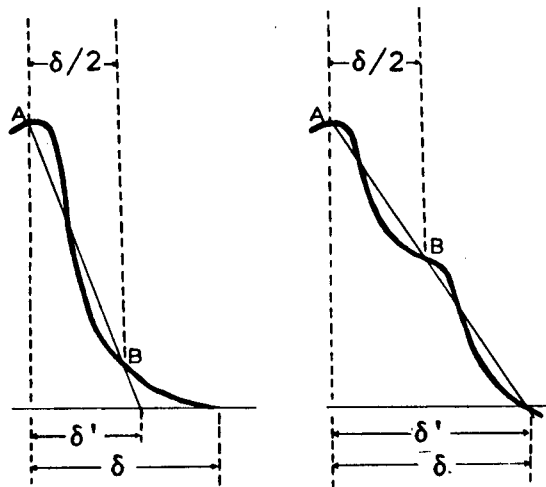
Figure 23 Pseudo duration used by Gotman et al. A pseudo duration, δ', is obtained by drawing a line from the half wave apex, A, through the point B on the waveform.
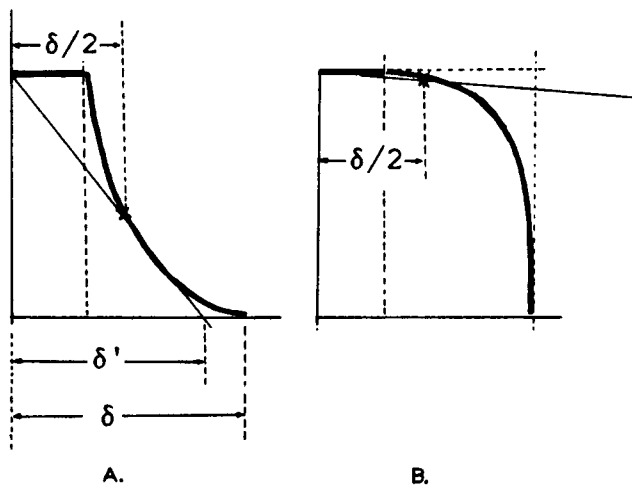
Figure 24 Halfwave Modelled by a hyperbola.
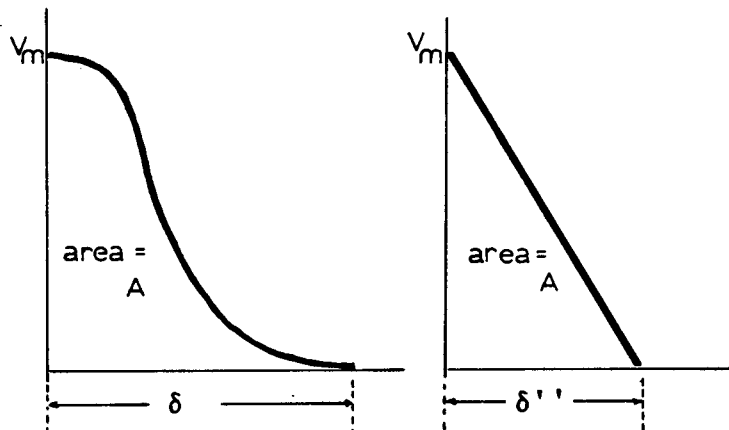
Figure 25 Area Matching Approach for Pseudo Duration. A pseudo duration, δ'', is obtained by matching the actual halfwave of area, A, amplitude, Vm, and duration, δ, with a triangular halfwave of the same area and amplitude but duration δ''.

4.4.2 Form Factor

In the presence of muscle artifact it is possible to get false detections that look nothing like SSW (see figure 26). Such false detections are easily eliminated by demanding a minimum of monotonicity on the rising and falling phases of the spike.

Consider the rising slope in figure 27 and let,

$$\Delta_1 = \sum_{n=0}^{N-1} |x_{n+1} - x_n| \qquad \qquad ...4.14$$

which is the sum of absolute differences of adjacent samples from A_1 to A_2.

Let,

$$\Delta_2 = |x_{N-1} - x_0| \qquad \qquad ...4.15$$

Then, as a 'form factor' we have that,

$$\eta = (\Delta_1 + \Delta_2) / \Delta_2 \qquad \qquad ...4.16$$

This measure will pass many types of shapes (see figure 28). It is a crude measure of higher frequency noise which is superimposed on the waveform.

Figure 26 Waveform With Superimposed muscle artifact.
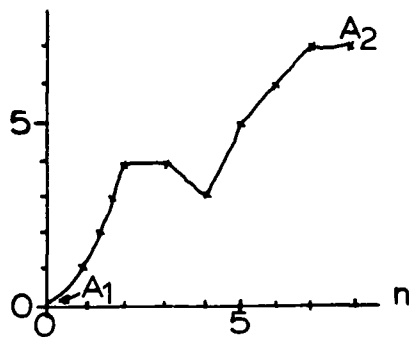
Δ_1 = sum of absolute differences = 1+3+0+1+2+1+1+0 = 9

Δ_2 = height of the halfwave = 7

η = form factor = $(\Delta_1 + \Delta_1)/\Delta_2$ = 2/7

Figure 27 Form Factor Computation.
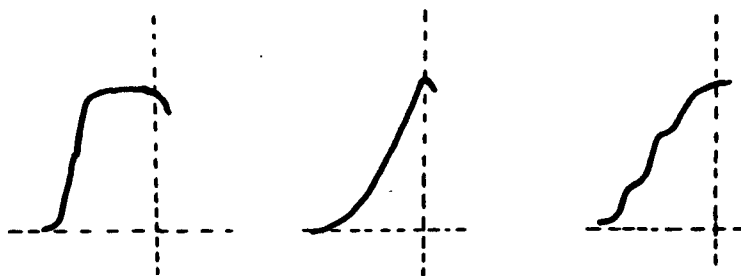
Figure 28 Different Waveforms with equal Form Factor.

4.4.3 <u>Triangularity</u>

None of the shape measures so far mentioned is useful in rejecting those waveforms with sharp rising and falling phases but flat or squared tops. Using the area measure discussed in the section on pseudo duration, it is possible to define a measure which gives some indication. We are interested in rejecting waves as seen in figure 29. If A = total area under the half wave and A' = area under the triangle only

then

$$T = (A - A') / A'$$

where T gives a measure of divergence from the ideal. There are several cases (figure 30) which can pass these simple tests, but are still quite different from the ideal. With these tests, however, we eliminate a large category of false detections with relatively simple algorithms.
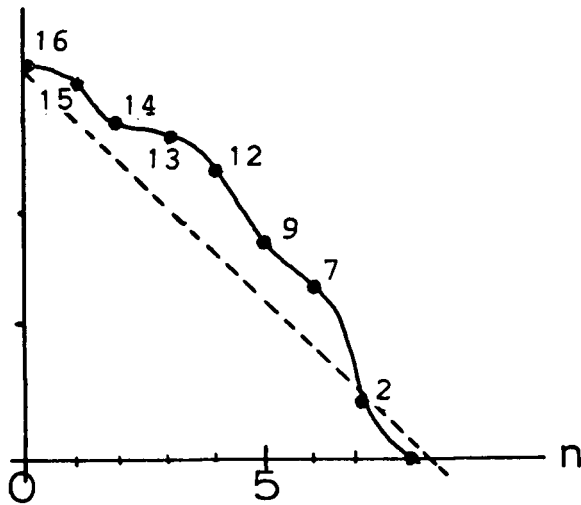
A = the area under the halfwave
    = 80

A'= the area under the triangle
    = 64

Υ = triangularity divergence
    = (80-64)/64 = .25

Figure 29 Triangularity Measure.
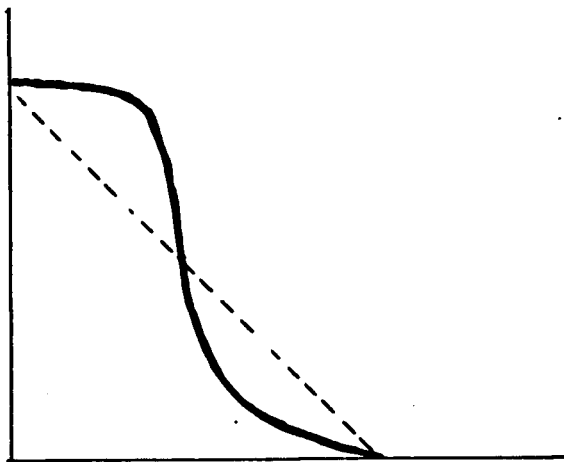
Figure 30 Non-ideal Waveform Which Passes the tests.

4.5 Artifact Rejection

It is possible to obtain waveforms which are similar to SSW but are generated by non-epileptic processes, artificial or otherwise. Distinguishing these from SSW requires that the context be considered, ie. we must look at the type of background or what the activity is like in the other channels. SSW rarely occur in only one channel. Thus, we can demand that there be simultaneous detections on several channels before an SSW is accepted. Unfortunately, with certain types of artifact, the events causing the false detection (ie. electrode pops) extend to more than one channel and other approaches must be used.

4.5.1 Movement Artifact

Patient movement causes the most severe disturbances in EEG recording (see figure 31). During periods of movement it is best not to attempt to detect SSW at all due to the heavy corruption of the signal. To ignore sections containing a lot of artifact, it is necessary to be able to detect the artifact. Since high frequency EMG is present during patient movement, it is a good flag for corrupting artifact.

The simple difference operator, $x(n) - x(n-1)$, can be used to detect muscle activity. It is a high pass operator with a frequency response, F_5, as shown in figure 32. The measure, Ψ,

in equation 4.17 is an indicator of muscle activity in the
signal. With this measure, no calibration procedure is
required.

$$\Psi(f) = (\ |F_5|^2 - |F_1|^2 \ ) \ / \ |F_5|^2 \qquad \ldots 4.17$$

The measure is not difficult to obtain using the relation
4.11 discussed earlier. $\Psi(f)$ ranges from 0 to 1. It is 0 when
$|F_1|$ and $|F_5|$ are equal (ie. not much power above 10hz) and 1
when $|F_5|$ is much greater than $|F_1|$.
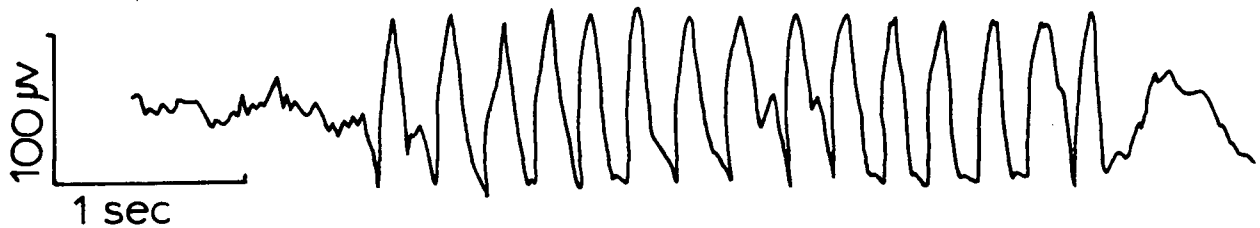
Figure 31 Effect of Patient Movement on EEG.
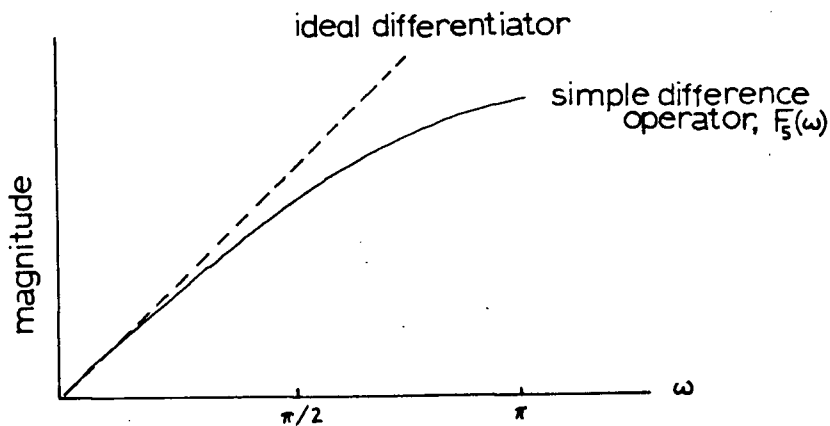
Figure 32 Magnitude Response of Simple Difference Operator, F_5.

4.5.2 Spindles And Alpha Rhythms

There are some typical rhythms which have similar shape and duration to spikes. Both alpha rhythms and sleep spindles can cause false detections. The threshold value of the bandpass output is set according to background statistics but this doesn't help if the rhythms come in short bursts (3 or 4 waves). The simplest approach is to detect the rhythms themselves and not to allow spike detections during the period when rhythms are present. Simple period measurements are effective in detecting the presence of these rhythms.

4.6 Phase Reversal Detection

In the case of focal epilepsy, determination of the location of a potential maximum is of special interest. If recording is bipolar, it is not straight forward where the maximum is. Consider the figure 33a. If recording is differential between electrodes A & B and B & C as shown, then if a potential maximum occurs at electrode B, we will obtain SSW in channel A-B and B-C but they will be reversed in phase. In figure 33b the potential maximum midway between electrodes B and C causes SSW of opposite polarity in A-B and C-D and none in B-C.

Since there are many montages, locating phase reversals and the areas of potential maximum is difficult. The task is made

more tractable if the montage is divided into bipolar chains (figure 34).

In designing an algorithm for phase reversal detection, the following conditions are imposed:

(1) SSW are considered for phase reversing if their apexes are shifted no more than 10 milliseconds in time.

(2) We consider bipolar chains with a maximum of seven channels.

(3) We consider chains with a minimum of 2 channels.

(4) Only 3 adjacent channels are considered at a time.

(5) Only one phase reversal is allowed per chain except in the case where the detected reversals are in homologous areas of the brain.

(6) There is a maximum of four chains in a given montage.

These restrictions are lenient enough to allow for detection of phase reversals in all the popular montages. The algorithm first divides the montage into separate chains and processes the chains in subchains of 3 channels. Currently, we are capable of handling 8 different montages but the main subroutines are general enough that other montages can be added as long as some information about the number and kind of chains is provided.
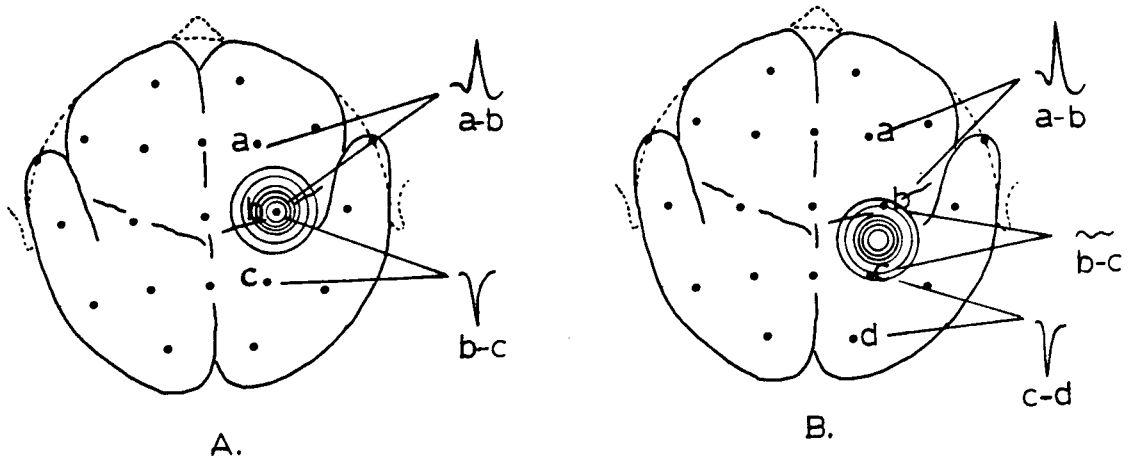
Figure 33 Examples of Phase Reversing.
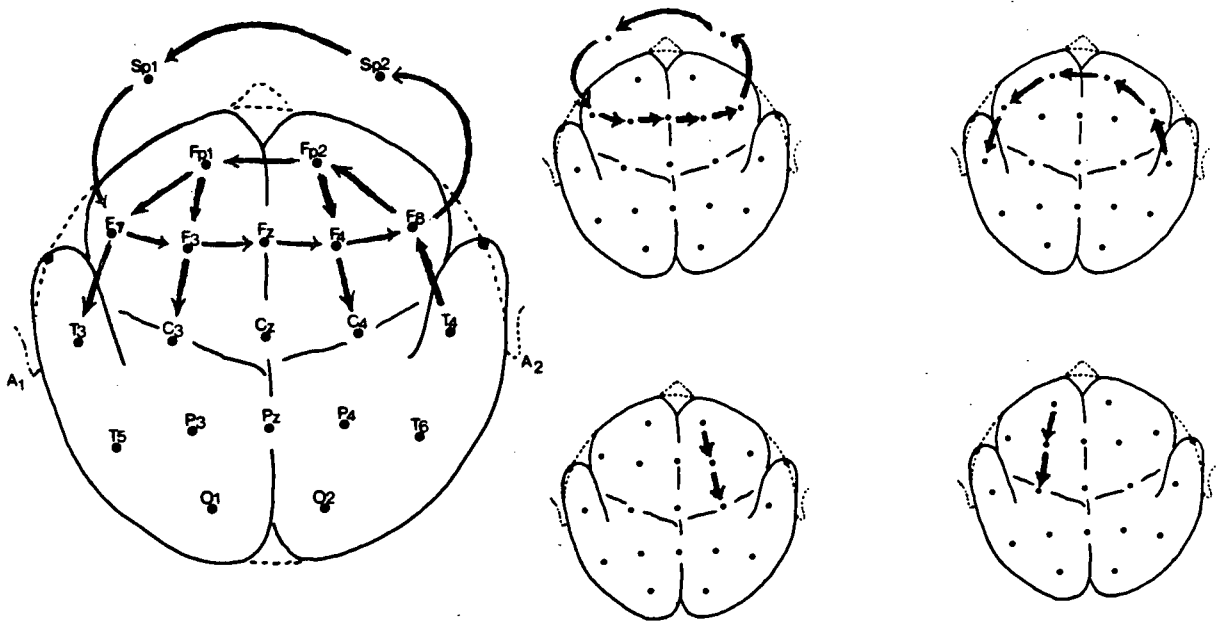
Figure 34 Bipolar Chains.

V. DETECTION OF SEIZURE ACTIVITY IN EEG

Apart from systems for spike and wave detection, there are very few reports of automated seizure detection systems. The only consistent work reported is by the team of Gotman et al[10 17 18] who have incorporated automatic seizure detection into their monitoring unit at the Montreal Neurological Institute (MNI). In this chapter, we will examine some features of seizures which can aid in their detection by computer. Later, we describe an approach used by us in the seizure monitor at the University of British Columbia.

The first reported automatic seizure monitor at the MNI employed a PDP-12 minicomputer and operated on eight channels of EEG in real-time. Seizure detection depended on the amplitude of the EEG and the output of a bandpass filter. The MNI system has since been redeveloped and the seizure detection system is part of an integrated system which also includes detection of interictal activity. Seizure detection criteria have been changed. The system does not attempt to detect all seizure activity; only that in which there is sustained paroxysmal activity with a fundamental frequency between 3 and 20 hz.

In a recent study of frequency content of EEG at seizure onset by the Gotman team[13] the fundamental seizure rhythm was most often found to be in the 3 to 6 or the 15 to 20 hz range (figure 35). In our own study of the frequency characteristics of EEG at seizure onset we found the same concentration of

fundamental seizure rhythms in the 3 to 6 hz range as the Gotman team, but we had no seizures with fundamental frequency in the higher range (figure 36). We were only able to study 1/3 the number of seizures that the Gotman group considered, and, unlike them, we included seizures corrupted by EMG artifact. Considering the problem of EMG obscurring higher frequency rhythms and the normally lower level of cerebral activity in the higher frequencies, that we found no higher frequency fundamental rhythms in the seizures we studied is therefore not surprising.

Initial results of seizure detection from the MNI system do not, at first, appear encouraging. From surface recordings, only 22% of the detections were of epileptiform activity and from depth recordings a mere 2.5% were true detections. False detections are not necessarily a problem, however, since the only function of their seizure detector is to trigger an EEG recording device so that a reduced amount of data can be examined later by an electroencephalographer. Even if the number of false detections is large, the amount of data reduction due to incorporating automated seizure detection is still significant.
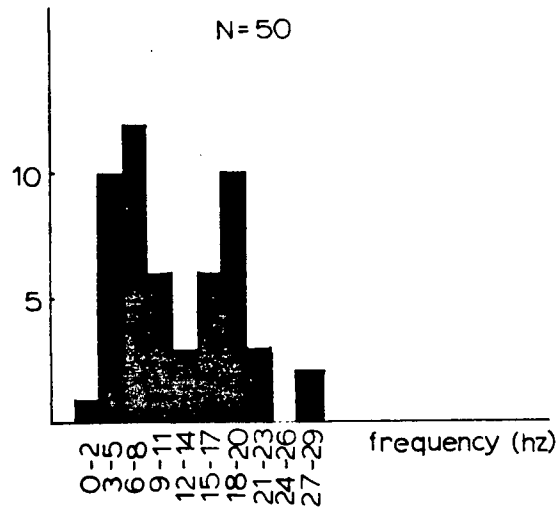
Figure 35 Fundamental Frequencies at Seizure Onset, I. The team of Gotman et al studied 50 seizures and recorded the fundamental frequency of the EEG activity at the seizure onset. Only seizures free of EMG activity were included in the study.
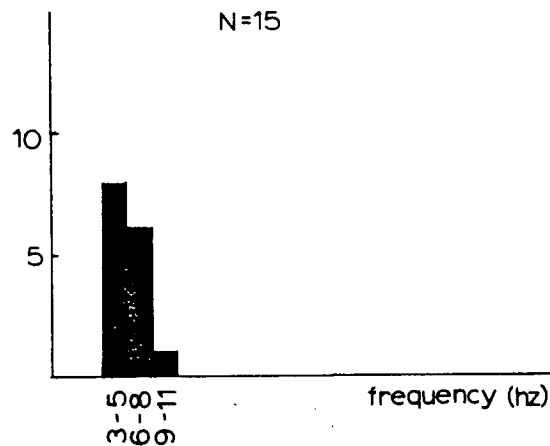
Figure 36 Fundamental Frequencies at Seizure Onset, II. At the UBC Hospital 15 seizures were studied and the fundamental frequency of the EEG at seizure onset was recorded. Seizures corrupted by EMG were included if there was a clear resonant peak in the spectrum.

In the Seizure Investigation Unit at the UBC Health Sciences Center Hospital we are developing a detector of seizure activity in EEG. Initially the goal has been limited to detecting seizures with moderate to high amplitude EEG activity. Such seizures are most often accompanied by clinical manifestations which, along with the EEG patterns at seizure onset are studied prior to a neurological diagnosis. A definition was provided by a neurologist that activity would be a candidate for seizure level activity if it was of high amplitude for a sustained period on a majority of the recording channels (figure 37). Sustained muscle activity could also be considered a sign of seizure.

An obvious approach was to put a threshold on the RMS value of the EEG as a detector of seizure level activity. Instead, the EEG is first filtered by a bandpass (the lowpass differentiator discussed earlier) and then the RMS value of the output is calculated. Motivation for use of the bandpass was rather simple: since interictal epileptiform activity was limited to a frequency range coincident with the pass band of the filter, the same might be expected of seizure activity. As the later frequency studies of seizures showed, the assumption of a direct correlation between the frequency distribution of SSW and of seizures was without justification. We did find, however, that at seizure onset there is a shift of signal power into the frequencies favored by the bandpass for most of the seizures studied. Several seizures were analysed as to their frequency content for several 5 second periods leading into the

beginning of the seizure. Two ratios were then calculated.

$$R1 = So / Si \qquad \qquad ...5.1$$

$$R2 = So' / Si' \qquad \qquad ...5.2$$

where So = EEG signal power after seizure onset, Si = EEG power before onset, So' = power of bandpassed EEG after seizure onset, and Si' = power of bandpassed EEG before onset. Eight seizures were studied and in 6 cases $R2 > R1$. In 1 case $R2 = R1$ and in only 1 case was $R1 > R2$. For the case where $R1 > R2$, $R2$ was still very much greater than 1.

The brief study mentioned here tends to support using a bandpass operator in the detection of seizures. The reason for the shift of signal power into the bandpass range is not clear. A large percentage of seizure records are corrupted by EMG. Gotman and Gloor estimate 30%, though our experience is that this figure is considerably higher (>50%). The bandpass will not entirely attenuate muscle activity, thus, this could be a partial explanation for the improvement gained by the bandpass. We have found, however, even in seizures that are free of EMG the relative shift of power into the bandpass range is still evident.

Following the bandpass operation, the signal is further processed. The RMS output of the bandpass is averaged over 5 second periods and it must pass a preset threshold to be considered of seizure level. The threshold must be passed in three successive, 5 second intervals and this must happen in a majority of the 16 channels or 3/4 of the channels of one

hemisphere. The requirement that activity be of a sufficient level on a number of channels reflects the fact that seizure activity comes to involve large sections of the brain. It is also possible that seizures remain confined to one hemisphere and, for this reason, each is also considered separately. Since the arrangement of channels varies from montage to montage, the detector had to be flexible enough to adapt to different ones.
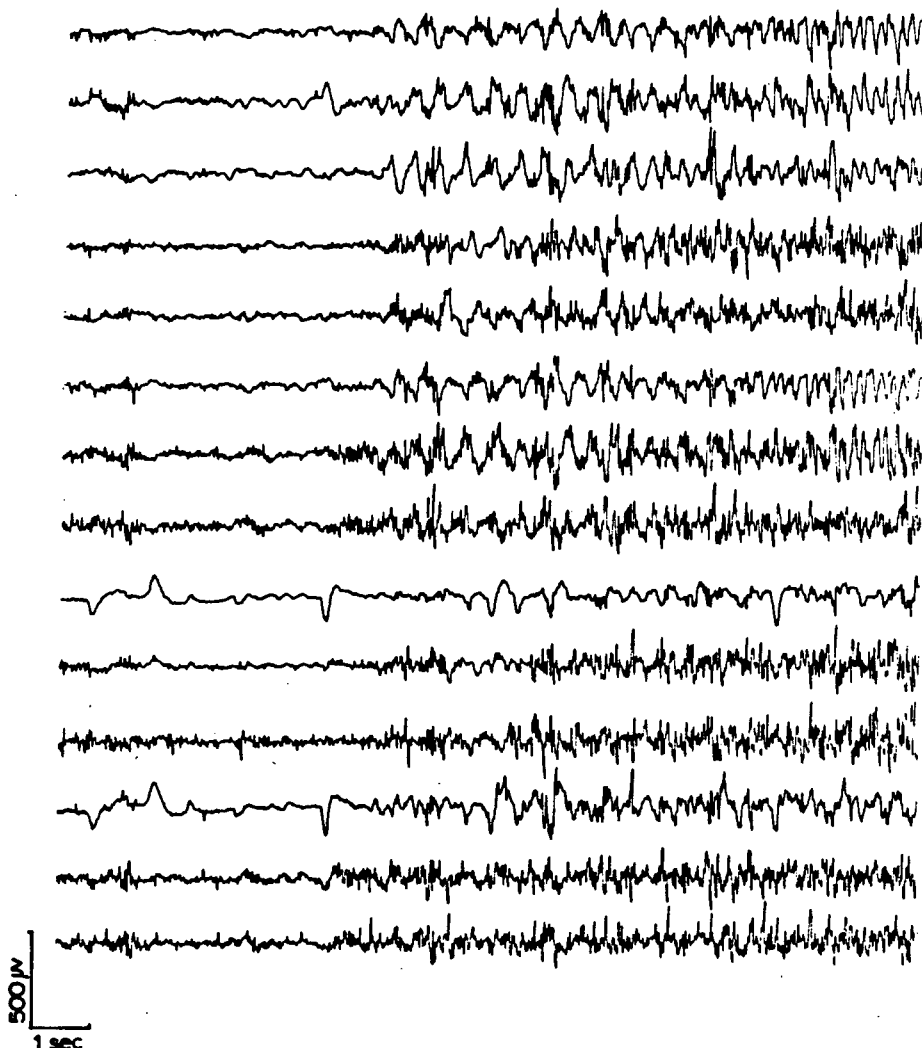
Figure 37 EEG at Seizure Onset. In many seizures the EEG signal level rises dramatically in most of the recording channels.

VI. IMPLEMENTATION OF THE EEG MONITOR

Many techniques for the detection of epileptiform activity in the human EEG are described in the literature. There are far fewer descriptions of integrated systems which incorporate these techniques into real-time monitoring devices. We will describe the implementation of an EEG monitoring system developed at the Seizure Investigation Unit of the University of British Columbia. Hardware schematics and software flowcharts can be found in the Appendix.

Our real-time monitor is comprised of a popular microprocessor system, some special purpose electronic hardware, and several software packages. The detection of seizures and detection of interictal activity is done by separate software modules, only one of which is resident in the system during a monitoring session. Only one patient is monitored at any given time.

6.1 Hardware Structure

Hardware for the EEG monitor constructed for use in the Seizure Investigation Unit of the UBC Acute Care Hospital consists of the units shown in figure 38. The basic pieces are a general purpose digital computer, color graphics monitor, and special purpose interface electronics.
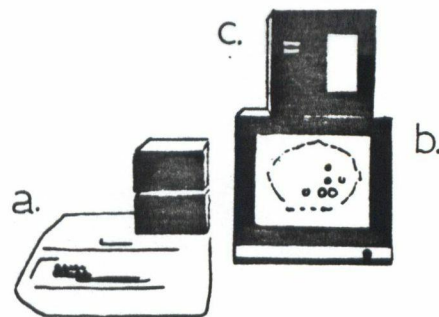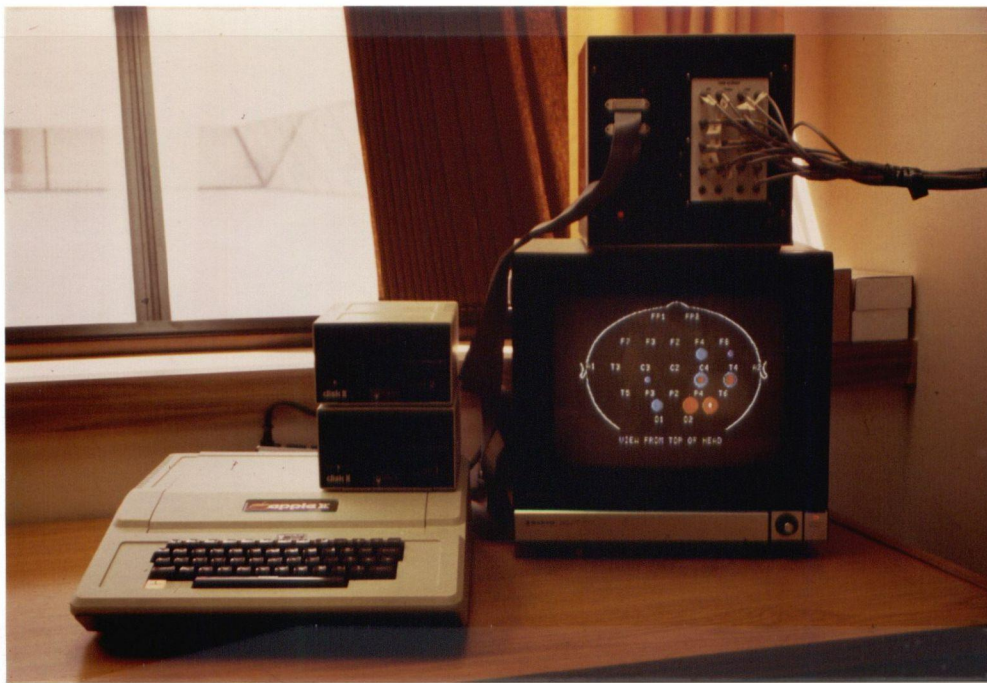
Figure 38   EEG   Monitor   Hardware   Components.   (a) Computer, (b) graphics monitor, and (c) interface electronics.

6.1.1 Computer Hardware

The computer is an Apple II Plus , a microprocessor-based device. Although developed for the home market, it is widely used for research and educational applications. The Apple II Plus is equipped with 48K bytes of random access memory on its main board. The machine includes a keyboard, power supply, circuitry for the generation of memory mapped graphics, system read only memory (ROM) with monitor and extended BASIC interpreter, special purpose I/O interface, and 8 expansion slots.

Five of the available 8 expansion slots are presently occupied by special purpose boards. There is a 16K byte memory expansion board, a timer board (which generates timed interrupts), a serial communications card, a disk controller (that can handle 2, 5 and 1/4 inch floppy disk drives), and an A/D-D/A board. All the peripheral boards, with the exception of the timer, were purchased off the shelf. The A/D board has 16 channels for analog to digital conversion (conversion time of 9 microseconds) and 16 channels for digital to analog conversion (conversion time of 16 microseconds). The conversion resolution is 8 bit. The timer board is software programmable and is enabled or disabled by commands which access specific location in the Apple's memory. A Sanyo color monitor is used for displaying text information and color graphics. All text and graphics are created by hardware which is inherent to the

computer. Input to the monitor is a single composite video signal generated by the computer.

6.1.2 Interface Hardware

A bank of filters and amplifiers was built to provide an interface between the EEG recording equipment and the A/D converter resident in the computer. A single order high pass filter with .1 hz cutoff removes very low frequency artifact. Fourth order Butterworth filters with a 25 hz corner frequency provide sufficient anti-aliasing for a 100hz sampling rate as well as 60 hz rejection of about 20db.

We have designed a special purpose board which includes low current relays that are opened by digital outputs included with the Apple. This board interfaces the Apple to a setup in the Seizure Investigation Unit for marking the audio tapes on which EEG is recorded. When the patient presses a (seizure) button a circuit is opened and the tape is marked so the EEG seizure record can be found later. Our interface is wired in series so that its relays can also open the circuit and mark the tape if the computer detects a seizure. Relays are used in order to provide total isolation of the computer from the rest of the equipment setup. The relay is held open by a monostable so that, even if the digital output of the computer is toggled by accident, the relay will only remain open momentarily and have minimal consequences in the operation of the seizure unit.

6.2 Monitor Software Structure

Monitor software is designed for (1) detecting and cataloging interictal SSW and (2) detecting seizures. As well as detection routines, there are programs for calibration, adjusting key system parameters, and maintaining patient files. All routines are loaded and started via a main menu program.

6.2.1 The SSW Monitor Software

The interictal monitor is written entirely in assembler, although its program modules are loaded and linked from a BASIC routine called from the main menu. On startup, the entire contents of the stack and zero page are relocated to a safe spot so that the monitor may make use of them without compromising the integrity of Applesoft BASIC or the disk operating system. On exit, the system is restored and the main menu program is re-entered.

The SSW monitor is interrupt driven - interrupts are generated at equal intervals according to the sampling rate desired (100hz). On each interrupt, conversions are made on each of 16 channels of incoming EEG and values are loaded into a buffer to await processing. Buffering is necessary so that the more complex processing, which is done on candidates from the first pass, can take several sample intervals. Samples are processed, one after the next, until the system buffer is empty.

Normally, spike candidates are few so that there is ample processing time. The buffer is large enough (4K bytes) to deal with short bursts of activity. In the unlikely case that the buffer overflows, the system turns off spike detection until enough space is available to continue.

The monitor consists of 4 tasks which run in parallel on three priority levels. The system accomodates multiple tasks at the middle priority level. Each task has its own section of stack and workspace to avoid conflicts over memory and resources. The running of tasks is organized by a task handling program. The 4 tasks, according to priority, are the following:

1) The Main Analysis Routine.

It is queued to run each time a new set of samples is placed in the signal buffer. It is the highest priority task in the system. As long as there are any samples left in the buffer, this task will continue to run, taking precedence over all tasks at other levels, even the interrupted tasks that are waiting to be restarted.

2) The User Inquiry Interface.

This task is queued to run in response to user inquiries about the system status. It is a level 2 task. Although the keyboard port is polled during the interrupt service routine, except for a few single character commands, response must wait according to the priority structure of the system.

3) The Graphics Routine.

This routine is queued to run every 1/4 of a second. It updates a continuous color graphics display (figure 39) of the results of SSW detection. This also is a priority level 2 task. If both task number 2 and number 3 are queued then number 2 will be run first, but task 3 must be run next. Also, any interrupted level 2 task takes priority over other level 2 tasks yet to be started.

4) The Background Task

This task is run when no task of any other kind is waiting. It has the lowest priority of all. At present, it does nothing but kill time. It is a nul task.
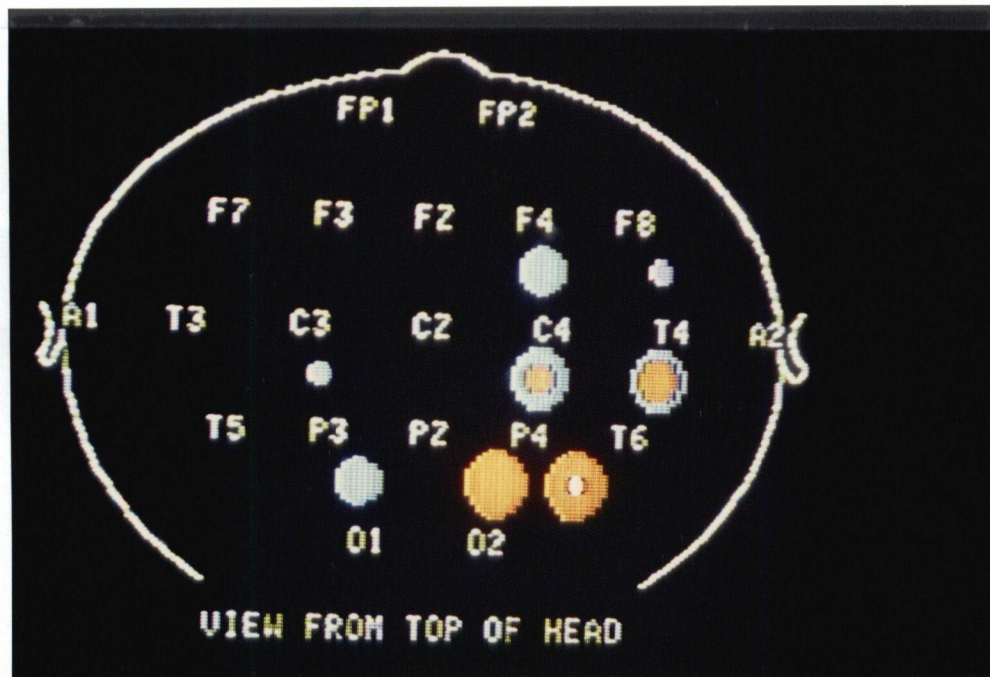
Figure 39 Color Graphics Display of SSW Monitor. The running sums of detected SSW are dynamically displayed using circles appropriately placed on a map of electrode locations. Sums are represented by both size and color of the circles.

6.2.2 The Seizure Monitor Software

The seizure monitor is also written in assembler, though it is loaded by a BASIC routine called by the menu program. Essentially, it is a subset of the spike monitor. The system structure is identical, although there is really only one task in the system. Other than the real time clock and a list of times of seizure detections, there is no graphics display.

When a seizure detection is made, the monitor marks the information (time) on the screen and holds a single digital output low for 1 second to signal the fact to the outside world. The output can be used to sound alarms, turn on recorders, etc. Presently, it is used to put a mark on the tape recording of the EEG.

VII. <u>RESULTS AND DISCUSSION</u>

In this chapter we evaluate the accuracy of the EEG monitor in detecting SSW and seizure activity. Evaluation of the seizure monitor is considerably easier than the SSW monitor. There are far fewer seizures and they are usually very dramatic events. It is , therefore, clear when the computer detects a seizure or misses it.

SSW are very short events. When they occur, it may be in great numbers. We are interested in the aggregate of the SSW detection and not so much in the detection of any single event. We may want to obtain totals simply to see if a certain drug has been effective in reducing the amount of abnormal activity. We may also want to use the information to aid in localizing the source of the abnormal activity.

7.1 Evaluation Of The SSW Monitor

As can be seen from figure 40, our simple detector is able to discriminate epileptiform activity from the background. Even in the case shown in figure 41, where the spike amplitude is lower than the background, a detection is made. When the EEG is relatively free from artifact the detection rate is quite good. There is a rate of better than 80% accurate detections with a false detection rate of less than 5%. When there is a great deal of artifact, particularly that due to movement, the rate of false detections can reach as much as 50% or more. The introduction of a muscle artifact detector has greatly reduced the rate of false detections but it has not completely eliminated the problem.

It is difficult to measure the effectiveness of the monitor on an event by event basis because of the vast amounts of data that are processed even over a short period of time. Instead, we have chosen to select a few patients and study the results of a monitoring session in relation to the neurological diagnosis. Three patients suffering from focal epilepsy were chosen. Results from 1 hour long monitoring periods were obtained and the results are shown in figures 42 to 44. The neurological diagnoses of the patients used in this study were based on the full time the patients were in the seizure investigation unit. This was several days in some cases. Because the computer monitoring was done only over short periods, some of the

activity analysed by the neurologist was not available to the computer.
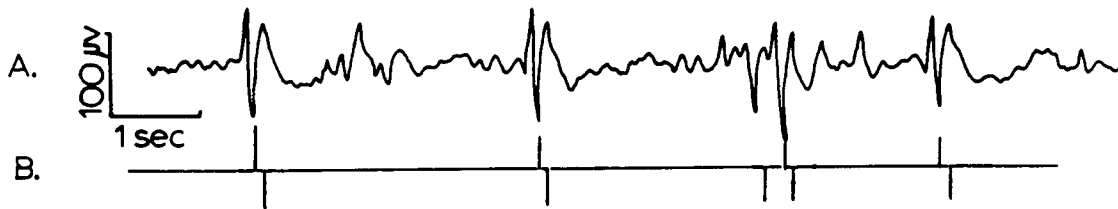
Figure 40 Detection of SSW. The bottom trace indicates where a detection is made.
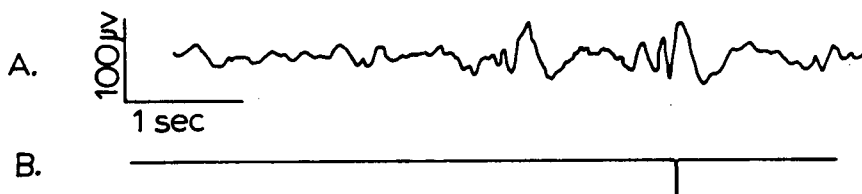
Figure 41 Detection of SSW; low signal to noise ratio. The bottom trace indicates where a detection is made.

Patient A was diagnosed as having multifocal epilepsy with one focus in the left occipital region and the other in the left temporal. Patient B has interictal abnormalities in the mesio-temporal region with a tendency to bilateralization and patient C has abnormal activity near the midline in the frontal region.

From the results presented in figures 42b, 43b, and 44b, we see that there is only a rough correlation between the neurological diagnosis and the SSW detection results. This is not surprising since, with bipolar recording montages, simple SSW information doesn't directly indicate the site of maximal activity. Phase reversal information is a more useful indicator of the site. It is also less susceptible to false detections since the criteria for phase reversal detection is quite stringent. In the following discussion we will rely primarily on the phase reversal detections for the evaluation of the SSW monitor.

From figure 42c we see a good correspondence between the plot of phase reversals and the neurological diagnosis (patient A). Both neurologist and computer note the existence of a focus in the left fronto-temporal region and a mirror focus on the right side. There is no sign of a focus in the left occipital region from the computer results as was noted by the neurologist. Unfortunately, no computer analysis was done of a montage covering that area. Therefore, it would not have been possible for the computer to predict the occipital focus.

Bipolar Channel Number	Electrode Pair
1.	$F_4 - F_z$
2.	$F_8 - F_4$
3.	$Sp_2 - F_8$
4.	$Sp_1 - Sp_2$
5.	$F_7 - Sp_1$
6.	$F_3 - F_7$
7.	$Fz - F_3$
8.	$F_8 - T_4$
9.	$Fp_2 - F_8$
10.	$Fp_1 - Fp_2$
11.	$F_7 - Fp_1$
12.	$T_3 - F_7$
13.	$F_4 - Fp_2$
14.	$C_4 - F_4$
15.	$F_3 - Fp_1$
16.	$C_3 - F_3$
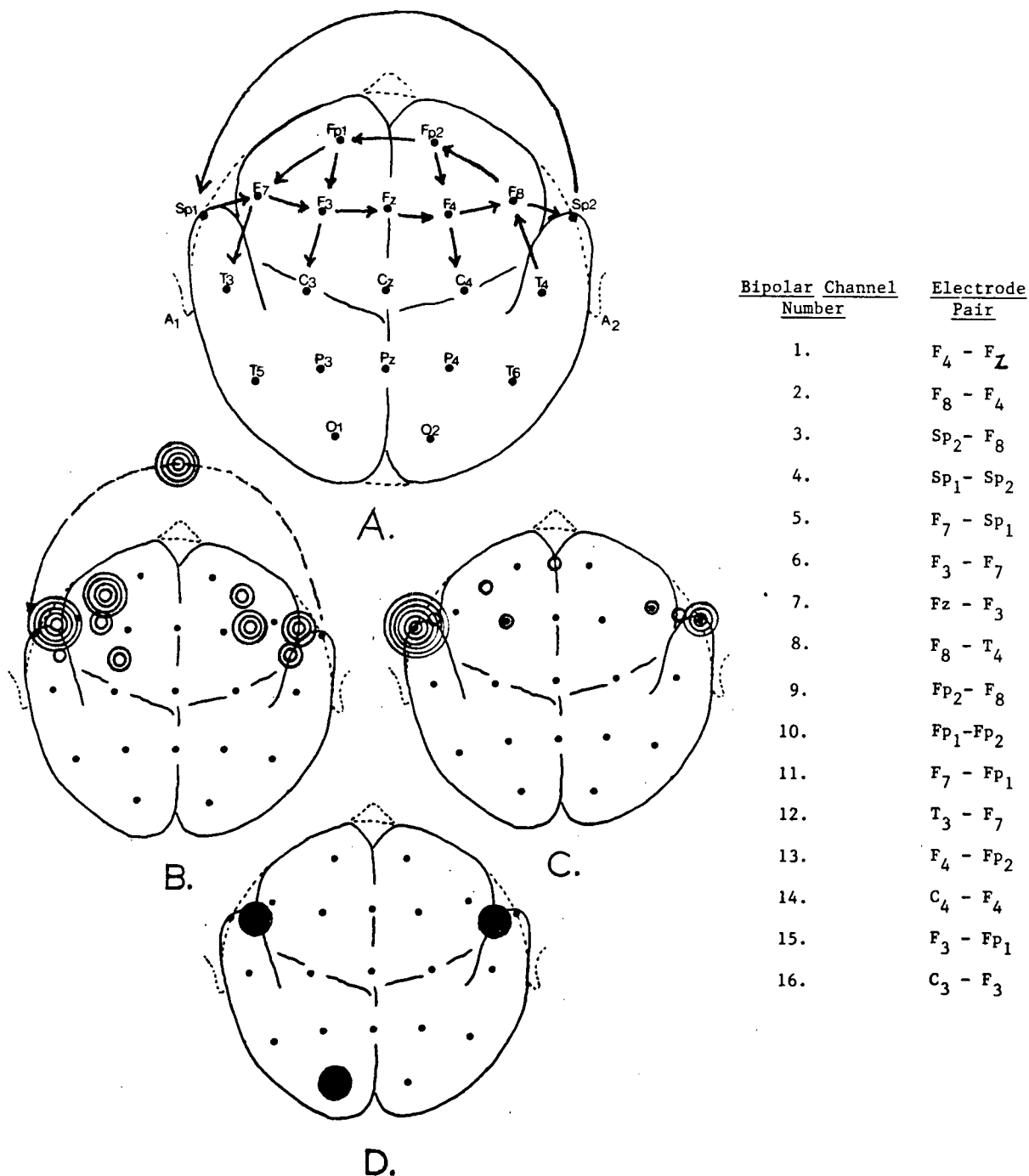
Figure 42 Interictal Monitoring; Patient A. (a) Montage used in monitoring. (b) Interictal SSW detection totals for Patient A (1 circle = 3 detected SSW). (c) Phase reversal totals for the same patient (1 circle = 1 phase reversal detected). (d) The locations are marked where patient A has multiple focii according to the neurologist. One focus is the left fronto-temporal region has a mirror focus on the right side. The neurologist also noted a focus in the left occipital region.

Patient B (figure 43) exhibits abnormal activity near the midline of the frontal region. The very large number of phase reversals detected in this area again indicates a good correspondence of the computer's results and the neurological diagnosis. The computer detected a large number of SSW in channel 13. When SSW occur at the ends of a bipolar chain, the monitor makes a special note of it because it could mean that there is a potential maximum at the last electrode in the chain. Information in these channels is similar to that obtained from phase reversals. SSW which appear alone at the end of a chain are sometimes considered phase reversals for this reason, even though there is no actual phase reversal in the chain. Since these types of 'phase reversals' only require the detection of a single SSW, they are more likely to be false detections and we must be careful when interpreting the results.

In the case of patient B, the detection of a large number of end-of-chain phase reversals at Fp2 (channel 13) has some significance since we have detected a number of phase reversals at the midline nearby. There were no phase reversals detected at Fp2 involving channels 9 and 10 as would be expected if indeed there was a strong potential maximum at Fp2. Therefore, the SSW detected in channel 13 are more likely due to a potential maximum near the midline rather than at Fp2. Since there are far more SSW in channel 13 on the right than in channel 15 on the left, however, we would expect that the activity is more lateralized to the right side of the midline. In fact, the neurological report mentions frontal abnormality

near the midline. There is some tendency to bilateralization, which coincides with our detection of a smaller number of SSW and reversals in the left frontal region.

There were a number of phase reversals detected around the sphenoidal electrode, Sp2. The neurological report makes no mention of this, but it seems the report was based primarily on slow wave analysis. Extensive damage was done in the frontal region of the patient's brain due to the entry of a small bullet, still lodged in the supra ventricle. It is, therefore, quite possible that abnormal activity would be coming from around Sp2. There is also the same tendency to bilateralization at the sphenoidal electrodes with a maximum occurring on the right side. This would further indicate that the reversals detected there are not merely due to artifact.

Bipolar Channel Number	Electrode Pair
1.	$F_4 - F_z$
2.	$F_8 - F_4$
3.	$Sp_2 - F_8$
4.	$Sp_1 - Sp_2$
5.	$F_7 - Sp_1$
6.	$F_3 - F_7$
7.	$Fz - F_3$
8.	$F_8 - T_4$
9.	$Fp_2 - F_8$
10.	$Fp_1 - Fp_2$
11.	$F_7 - Fp_1$
12.	$T_3 - F_7$
13.	$F_4 - Fp_2$
14.	$C_4 - F_4$
15.	$F_3 - Fp_1$
16.	$C_3 - F_3$
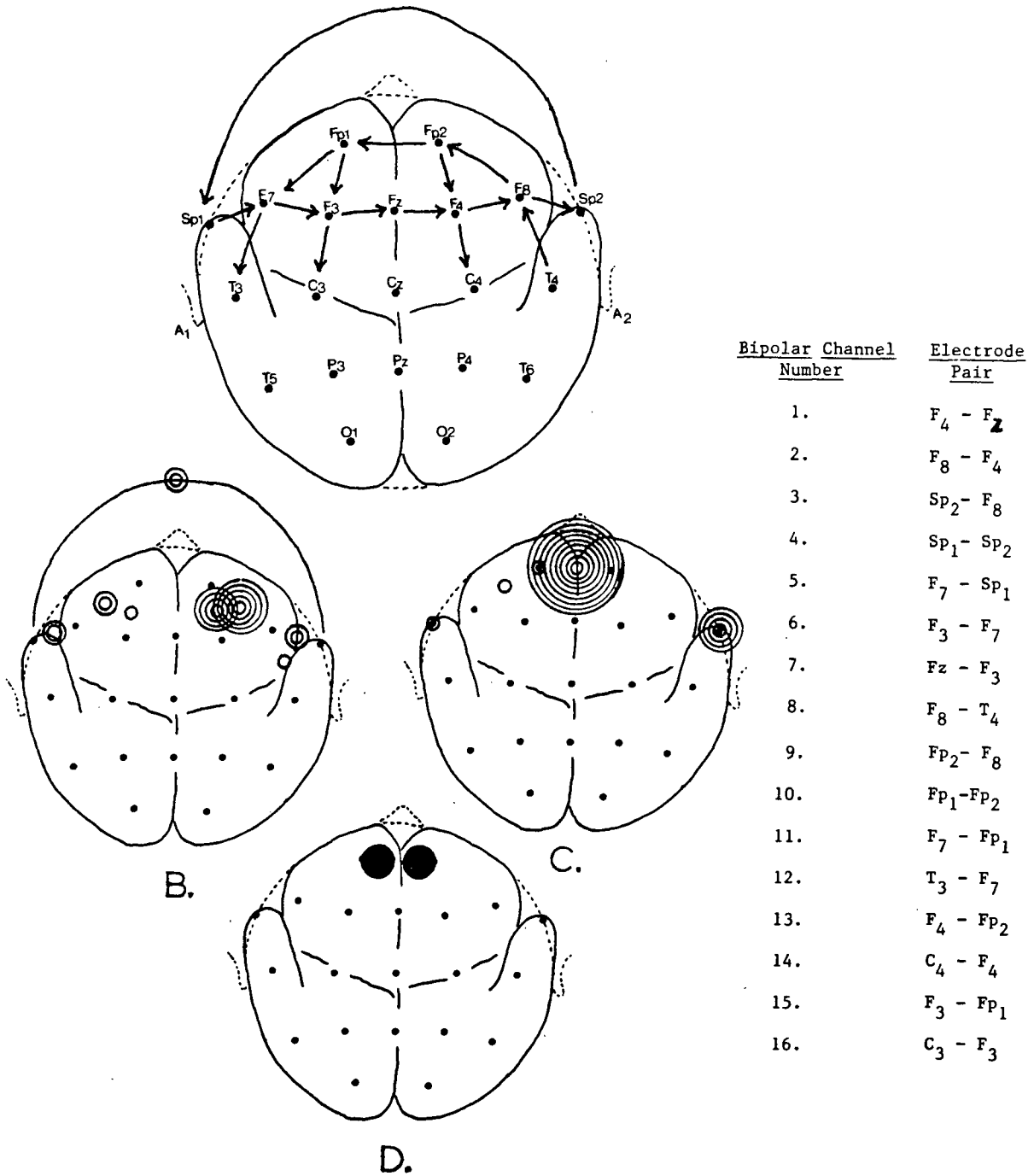
Figure 43 Interictal Monitoring; Patient B. (a) Montage used in monitoring. (b) Interictal SSW detection totals for Patient B (1 circle = 10 SSW detected). (c) Phase reversal totals for the same patient (1 circle = 1 phase reversal detected). (d)The locations are marked where, according to the neurologist, patient B exhibits abnormal activity. This is near the midline in the frontal region. There is right frontal activity near the midline with some tendency to bilateralization.

Patient C exhibited interictal activity in the anterior mesio-temporal area. There was a tendency to independent bilateralization. Looking at figure 44c, we see that reversals were detected near the sphenoidal electrodes Sp1 and Sp2. Considering that the exact location of the surgically implanted sphenoidal electrodes is difficult to determine, the computer prediction is reasonable.

The report also mentions that activity is greater on the left side than on the right but the computer detected more phase reversals on the right side. If we look at figure 44b, however, the picture is somewhat different. There are a considerable number of SSW at the ends of bipolar chains in channels 1,5,6, and 10. The computer determined that most of these represented end-of-chain phase reversals. It is probable that many are bona fide potential maxima at the ends of their respective bipolar chains. Many more of them were detected on the left than on the right which would agree with the findings of the neurologist.

Bipolar Channel Number	Electrode Pair
1.	$F_8 - F_4$
2.	$Sp_2 - F_8$
3.	$Sp_1 - Sp_2$
4.	$F_7 - Sp_1$
5.	$F_3 - F_7$
6.	$T_4 - C_4$
7.	$Sp_2 - T_4$
8.	$Sp_1 - Sp_2$
9.	$T_3 - Sp_1$
10.	$C_3 - T_3$
11.	$F_8 - Fp_2$
12.	$T_4 - F_8$
13.	$T_6 - T_4$
14.	$F_7 - Fp_1$
15.	$T_3 - F_7$
16.	$T_5 - T_3$
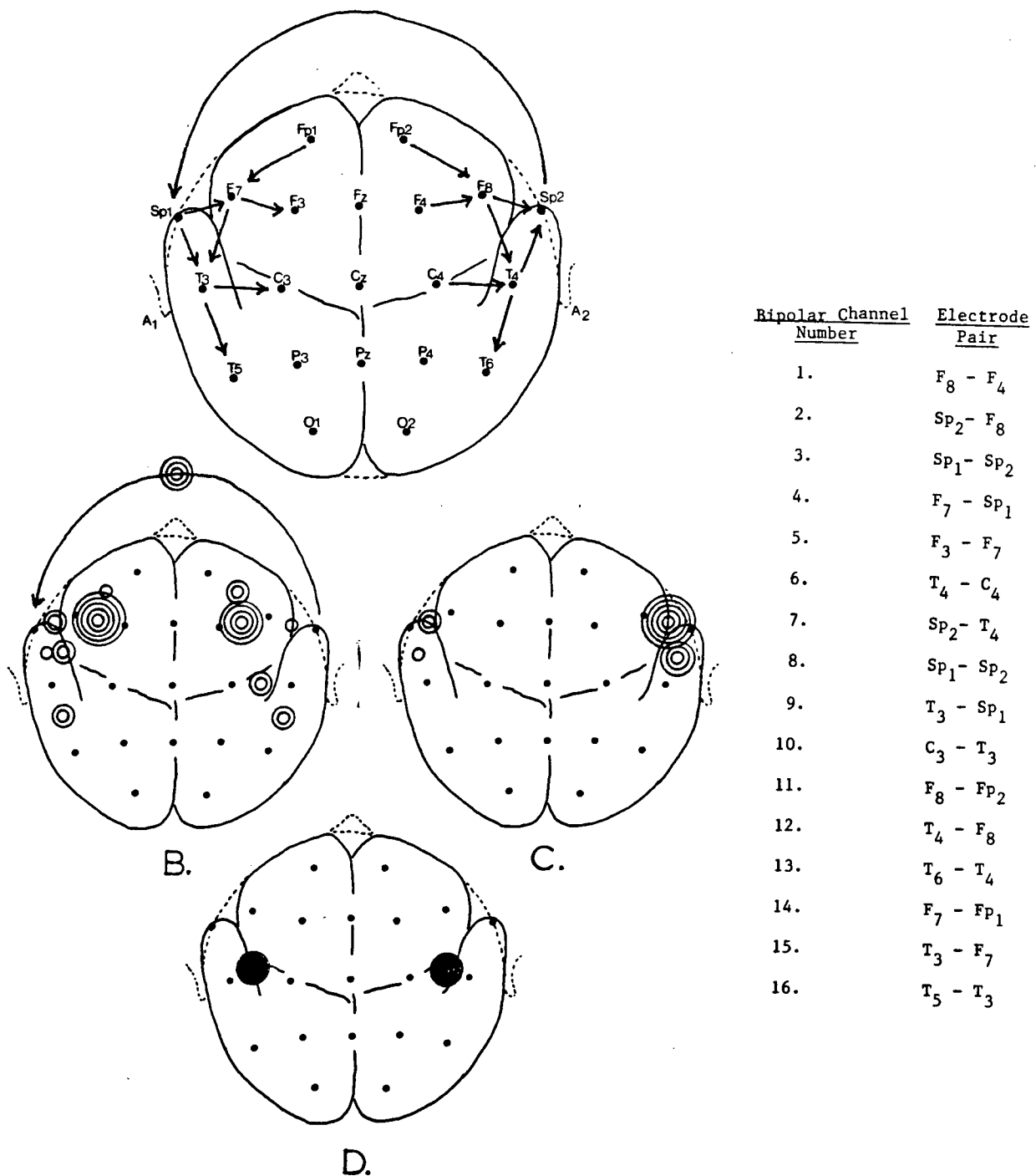
Figure 44 Interictal Monitoring; Patient C. (a) Montage used in monitoring. (b) Interictal SSW detection totals for Patient C (1 circle = 6 SSW detected). (c) Phase reversal totals for the same patient (1 circle = 1 phase reversal detected). (d)The locations are marked where, according the the neurologist, Patient C exhibits abnormal activity. This is in the mesio-temporal region. There is a tendency to independent bilateralization.

From this brief study, we can see that the interictal SSW monitor, at its present stage of development, is capable of predicting the focus or focii of activity which correlate quite well with the findings of a neurologist. In one of the cases presented here (patient B) the monitoring session included several lengthy periods of corrupting muscle and movement artifact. In spite of the artifact, we were able to get results which corresponded well with the findings of the neurologist.

In order to insure the acceptance of a large enough percentage of actual SSW (ie. a small false rest probability), we usually end up with a large number of candidates from the first pass of the detection algorithm. That number is greatly reduced by subsequent processing but we still can have a high level of false detections in the presence of serious artifact. For long term recording sessions this is not good enough. At present, the results are obtained from 1 hour recording sessions with an operator in attendance. The dynamic graphics display lets the operator know how well the monitor is doing so that, if there are long segments with false detections, the session can be aborted.

A goal for future development of the monitor should be to reduce the rate of false detections. The strategy for achieving this is twofold. First, although we have included some tests of SSW shape, we have not exploited all that is known about SSW morphology in the detection algorithm. Second, we must develop better artifact detectors. Detecting the presence of muscle

artifact has aided in reducing false detections but some movement and electrode artifact continues to be problematic. Developing detectors (for SSW or artifact) requires the ability to identify enough useful parameters of the waveforms to discriminate them from normal activity. Identification of such parameters ultimately involves the analysis of large amounts of data from a large number of patients.

7.2 Evaluation Of The Seizure Monitor

The EEG seizure monitor, although still in a developmental state, has been in operation in the Seizure Investigation Unit for some time. This has made it possible to obtain a good measure of its performance. Over the period of 6 months, the seizure monitor was operating almost continually. Because we are still unable to monitor both patients in the unit at the same time, we were only able to obtain results from about half the patients who went through the unit. Of these, a few had no seizures at all. In total, we have results from 12 different patients and these are shown in table I.

The requirements of seizure detection are different from SSW detection. The goal is to detect seizures but, since we only want to signal their occurrence for later scrutiny by humans, we can tolerate a relatively high degree of false detections. Missing a few interictal SSW is not of much consequence since generally there are a lot of them. This is not true of seizures. If at all possible, we want to detect 100% of the seizures because there are so few of them. We aim for a perfect rate of detection even at the expense of a higher rate of false detections.

Number of patients 12

Total number of seizures 30

Total number of detections
      by the computer 54

Total number of false detections
      by the computer 26

Total number of true detections
      by the computer 28

Total number of seizures missed
      by the computer   2

Total number of seizures detected only
      by the computer 11

TABLE I Automatic Detection of Seizures. Results of computer detection of seizures in the Seizure Investigation Unit for a period of 6 months beginning November 1982.

From the results presented in Table I, we see that, of 54 computer seizure detections, 52% were bona fide seizures and 48% were false detections. The rate of false detections is quite acceptable. It means that for every two seizures the computer detects, one is valid. This is an enormous saving in time for the human observer, considering that the alternative is to study the EEG record for the entire monitoring period.

The relatively low rate of false detections can only be considered good if the rate of false rests in very low or 0. In fact, in 30 valid seizures the computer missed 2 (from the same patient) of them or only 7%. We should also look at the number that would have been missed without computer monitoring. Some 11 seizures, or 37% of the total number, would have gone

undetected if not for the computer monitoring. Comparing this with the 7% of the misses by the computer, the monitor seems very good. Since the monitor was active roughly twice as long as there were human observers available to detect the computer's misses, however, we could expect the actual false rest rate to be almost double at around 13%.

The seizures that were missed did not conform to the definition we were working with - moderate to high amplitude activity on a majority of channels. That we missed some seizures is, therefore, more a shortcoming of our original definition of a seizure that it is a problem of the detector. The original definition is sufficient for most clinically significant seizures, however, there are seizures of interest to the medical staff which are not being detected. The main distinguishing feature of the seizures missed by the computer is a strong rhythmic content on most channels. It is not necessary to include a capability for sophistocated frequency analysis to detect such seizure rhythms. A simple analysis, which gives the average period and the amount of deviation from the average would be sufficient. The interictal monitor already uses this technique in detecting alpha rhythms, although in that case we only look at very short sections of the waveform (4 periods). In seizure detection, we are only interested in rhythms that are sustained over a long time (in excess of 5 seconds) and are on many channels.

In this chapter we have evaluated the effectiveness of the EEG monitor to detect SSW and seizures. For both monitors the evaluation indicates the need for further development. This is particularly true for the interictal monitor. We have shown, though, that both monitors give very positive results. The seizure monitor is already in use in the Seizure Investigation Unit and the interictal SSW monitor, if used subject to some restrictions, can also extract useful information.

VIII. SUMMARY

We have described the development of a real-time EEG processor to be used for patient monitoring in the Seizure Investigation Unit of the Acute Care Hospital at the University of British Columbia. This monitor automatically detects epileptiform abnormalities in patient EEG as an aid in neurological diagnosis. Both seizure and between seizure activity are targets of the investigation.

The seizure detector operates with a definition of seizure level activity as that which is of consistently high amplitude on a majority of recording channels. The definition is not sufficient to detect all seizures but is sufficient to flag most clinically significant ones. The EEG is first subjected to a bandpass operation, because we have found that, at the onset of seizure, signal power shifts into the range of frequencies favored by the band pass filter. A seizure is detected when the output power of the bandpassed signal reaches a threshold level on a majority of all channels or 3/4 of the channels in one hemisphere.

Initial results of seizure detections are encouraging. Over 90% of seizures occurring during a 6 month period were accurately detected by computer in the Seizure Investigation Unit. The false alarm rate was about 50% but this is considered acceptable since the purpose of the monitor is only to note the occurrence of the seizures for later verification by a

neurologist or electroencephalographer.

The EEG monitor is also designed to detect between seizure epileptiform activity known as spikes and sharp waves (SSW). These are short transient events of less than 250 milliseconds in duration whose main distinguishing feature is their relative sharpness compared to the background EEG. Many approaches have been tried in the automatic detection of SSW and these can be divided into two categories; parametric and non-parametric detectors. Non-parametric detectors attempt to match an ideal model of the SSW to the input waveforms. The model may be a template, a set of parameters, a set of rules, or some combination of all of these. Such detection methods, on some level, try to mimic the action of the human observer. The parametric approach assumes an ideal model of the background EEG. When the signal fails to conform to the model, it is assumed to be due to abnormal events such as SSW. There is no mimicing of the human in this approach. In fact, a parametric filter is apparently able to detect SSW otherwise invisible to the human eye. Considering the difficulty in exactly defining SSW, it therefore appears quite attractive as a detection scheme.

Our experience has been that, in practice, the parametric approach is no more effective than simpler non-parametric detectors. Using percentage gain in signal-to-noise ratio from input to output of a system as a measure of performance, we theoretically compared the inverse spectral filter (parametric

detector) to a simple bandpass filter (non-parametric detector) as SSW detectors. From a signal-to-noise point of view, we found no theoretical advantage of the inverse filter over the bandpass.

The parametric approach is to model the background EEG, but little is actually known about the mechanisms which generate EEG patterns. The non-parametric approach is to model the SSW, but definitions of SSW are vague. There are problems, therefore, with both approaches. The non-parametric methods are, however, generally much easier to implement and are almost always used in practical, real-time detection systems.

Our approach to SSW detection is to process EEG on a first pass with a low-level operator that discriminates SSW candidates on the basis of a sharpness criterion. The low-level operator is a bandpass filter. It acts as a good detector of SSW in EEG whose power is concentrated in lower frequencies. When higher frequency activity such as alpha rhythms or muscle artifact is present, SSW detection is disabled completely. Waveforms accepted on the first pass detection are then subjected to a series of tests based on their morphological characteristics.

The accuracy of the monitor for detecting SSW was evaluated by comparing results obtained from several computer monitoring sessions with the neurological diagnosis of 3 patients suffering from focal epilepsy. In all cases, in spite of some problems caused by artifact, the monitor was able to accurately predict the location of epileptic foci as noted by the neurologist.

Very positive results were obtained in detecting both seizure and between seizure activity. The EEG processor, therefore, has immediate value as a clinical device. Much of the epileptiform activity recorded is never viewed by the medical staff because of the impossibility of searching through all the data. Now, with the introduction of computer monitoring, data can be preprocessed to save only relevant information for later scrutiny by humans.

An immediate goal for future work is the improvement of the processor to minimize detection error. A further goal is to move beyond detection and attempt to answer some of the basic questions of the generation of epileptiform activity: Do SSW occur randomly in time or are they generated according to some deterministic pattern? What is the relationship, if any, between ictal and interictal activity? What significance is there to seizure rhythms? Can a model be developed for the generation of epileptiform activity? Providing answers to such questions requires the study of massive amounts of data. In the past, the ability to analyse data has been limited primarily by the lack of automated systems of analysis. Real-time, automatic, computer detection of epileptiform activity in EEG provides a strong base from which we can begin to tackle some of these puzzling questions.

REFERENCES

1. Barlow,John S.
   "EEG Transient Detection by Matched Inverse Digital
   Filtering"
   Electroencephalography and Clinical Neurophysiology
   1980,48:246-248

2. Barlow,John S.
   "Computerized Clinical Electroencephalography in
   Perspective"
   IEEE.T.BME No.7 July 1979 pp.377-388

3. Birkemeier,William P.   ,Fontaine,A.Burr ,Celesia,Gastone
   G.   ,and Ma,Ken M.
   "Pattern Recognition Techniques for the Detection of
   Epileptic Transients in EEG"
   IEEE.T-BME May 1978

4. Bodenstein,Gunter and Praetorius,H.Michael
   "Feature Extraction from Electroencephalogram by Adaptive
   Segmentation"
   Proc.IEEE Vol.65,No.5,May 1977,pp.642-652

5. Carrie,J.R.G.
   "A Hybrid Computer Technique for Detecting Sharp EEG
   Transients"
   ECN 1972,33:336-338

6. Chatrian,G.E.   ,Bergamini,L.   ,Dondey,M.   ,Klass,D.W.
   ,Lennox-Buchthal,M.   ,and Petersen,I.A.
   "Glossary of Terms Most Commonly Used by Clinical
   Electroencephalographers"
   ECN 1974,37:538-548

7. Cooper,R.   ,Osselton,J.W.   ,and Shaw,J.C.
   EEG Technology
   London:Butterworth 1969

8. Gevins,Alan S.   ,Yeager,Chas.L.   ,Diamond,S.L.
   ,Spire,Jean-Paul ,Zeitlin,Gerry M., and Gevins,Adria H.
   "Automated Analysis of the Electrical Activity of the
   Human Brain (EEG): A Progress Report"
   Proc.IEEE Vol.63 No.10,Oct.1975,pp.1382-97

9.   Gotman,J.
      "Quantitative Measurements of Epileptic Spike Morphology
      in the Human EEG"
      ECn 1980,48:551-557

10.   Gotman,J.
      "Automatic Recognition of Epileptic Seizures in the EEG"
      ECN 1982,54:530-540

11.   Gotman,J.   and Gloor,P.
      "Automatic Recognition and Quantification of Interictal
      Epileptic Activity in the Human Scalp EEG"
      ECN 1976,41:513-529

12.   Gotman,J.   ,Ives,J.R.   ,and Gloor,P.
      "Automatic Recognition of Interictal Epileptic Activity in
      Prolonged EEG Recordings"
      ECN 1979,46:510-520

13.   Gotman,J.   ,Ives,J.R.   ,and Gloor,P.
      "Frequency Content of EEG and EMG at Seizure Onset:
      Possibility of Removal of EMG Artifact by Digital
      Filtering"
      ECN 1981,52:626-639

14.   Guedes de Oliveira,Pedro H.H.   and Lopes da Silva,F.H.
      "A Topographical Display of Epileptiform Transients Based
      on a Statistical Approach"
      ECN 1980,48:710-714

15.   Gutman,Irwin ,Wilkes,S.S.   ,and Hunter,J.Stuart
      Introductory Engineering Statistics
      John Wiley and Sons, 1971

16.   Isaksson,Anders ,Wennberg,Arne ,and Zetterberg,Lars H.
      "Computer Analysis of EEG Signal with Parametric Models"
      Proc.IEEE Vol.69 No.4,Apr.1981,pp.451-461

17.   Ives,J.R.   and Gloor,P.
      "A Long-Term Time-Lapse Video System to Document the
      Patient's Spontaneous Clinical Seizure Synchronized with
      the EEG"
      ECN 1978,45:412-416

18. Ives,J.R. ,Thompson,C.J. ,and Gloor,P.
    "Seizure Monitoring: A New Tool in Electroencephalography"
    ECN 1976,41:422-427

19. Jasper,H. and Kershman,J.
    "Application of the EEG in Epilepsy"
    ECN 1949,1:123-131

20. Kooi,K.A.
    "Voltage-Time Characteristics of Spikes and Other Rapid
    Electroencephalographic Transients: Semantic and
    Morphological Considerations"
    Neurology (Minneapolis),1966,16:59-66

21. Lemieux,John F. and Blume,Warren T.
    "Automated Morphological Analysis of Spikes and Sharp
    Waves in Human Electrocortiograms"
    ECN 1983,55:45-50

22. Lieb,Jeffrey P. ,Woods,Stephen C. ,Siccardi,Antonio
    ,Crandall,Paul H. ,Walter,Donald O. ,and Leake,Barbara
    "Quantitative Analysis of Depth Spiking in Relation to
    Seizure Focii in Patients with Temporal Lobe Epilepsy"
    ECN 1978,44:641-663

23. Lopez da Silva,F.H. ,van Hulten,K. ,Lommen,J.G.
    ,van Leeuwen,W.Storm van Veelen,C.W.M. ,and
    Vliegenthart,W.
    "Automatic Detection and Localization of Epileptic Focii"
    ECN 1977,43:1-13

24. Lopez da Silva,F.H. ,ten Broeke,W. ,van Hulten,K. ,and
    Lommen,J.G.
    "EEG Non-Stationarities Detected by Inverse Filtering in
    Scalp and Cortical Recordings of Epileptics: Statistical
    Analysis and Display"
    Quantitative Analytic Studies in Epilepsy (ed)Kellaway and
    Pedersen, Raven Press,N.Y.1976

25. Ma,K.M. ,Celesia,G.G. ,and Birkemeier,W.P.
    "Non-Linear Boundaries for Differentiation Between
    Epileptic Transients and Background Activities in EEG"
   IEEE.T-BME May 1977 pp.288-290

26. Makhoul,John

"Linear Prediction: A Tutorial Review"
Proc.IEEE Vol.63,No.4,Apr.1975,pp.561-578

27. McEwan,James A. and Anderson,Grant B.
     "Modeling the Stationarity and Gaussianity of Spontaneous
     Electroencephalographic Activity" IEEE.T-BME Sept.1975

28. Michael,D. and Houchin,J.
     "Automatic EEG Analysis: A Segmentation Procedure Based on
     the Autocorrelation Function"
     ECN 1979,46:222-235

29. Ninomiya,Satoki ,Matsubara,Masako ,and Wada,Juhn
     "Automatic Spike Detection from Human EEG Record"
     MEDINFO'80 (ed)Lindberg/Kaihara

30. Pfurtscheller,G. and Fischer,G.
     "A New Approach to Spike Detection Using a Combination of
     Inverse and Matched Filter Techniques"
     ECN 1978,44:243-247

31. Pola,P. and Romagnoli,O.
     "Automatic Analysis of Interictal Epileptic Activity
     Related to its Morphological Aspects"
     ECN 1979,46:227-231

32. Raemer
     Statistical Communications - Theory and Applications
     Prentice Hall, 1969

33. Saltzberg,B. ,Lustick,L.S. ,and Heath,R.G.
     "Detection of Focal Depth Spiking in the Scalp EEG of
     Monkeys"
     ECN 1971,31:327-333

34. Smith,Jack R.
     "Automatic Analysis and Detection of EEG"
     IEEE T-BME Vol.BME-21,No.1 Jan.1974

35. Usui,Shiro and Amidror,Itzhak
     "Digital Low-Pass Differentiation for Biological Signal
     Processing"
     IEEE T-BME Vol.BME 29,No.10,Oct.1982

36. Vera,R.S. and Blume,W.T.
     "A Clinically Effective Spike Recognition Program: Its Use
     at Electrocortiography"
     ECN 1978,45:545-548

37. Walter,D.O. ,Miller,H.F. ,and Jell,R.M.
     "Semiautomatic Quantification of Sharpness of EEG
     Phenomenon"
     IEEE T-BME Jan.1973 pp.53-55

38. Webster,John G. and Cook,Albert M.
     Clinical Engineering; Principles and Practices
     Prentice Hall, 1979

39. Epilepsy International Symposium
     Vancouver, B.C., Canada September 1978

APPENDIX A - SPECIALLY CONSTRUCTED HARDWARE
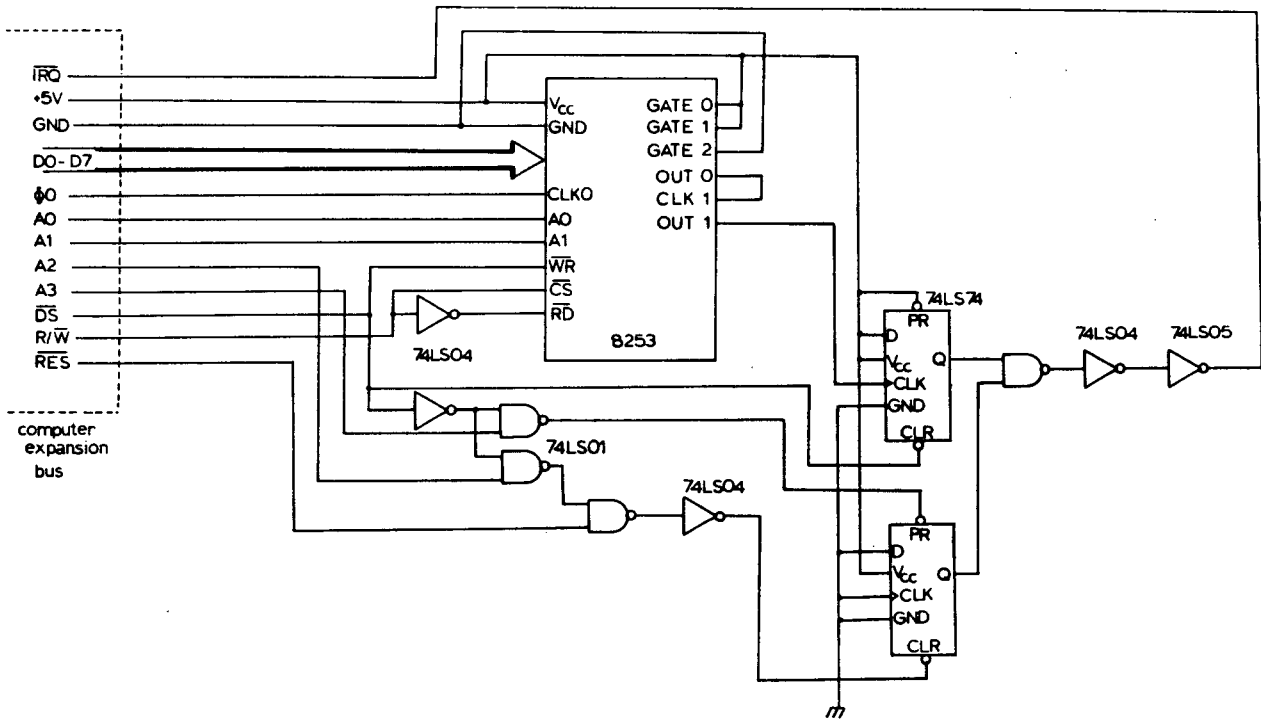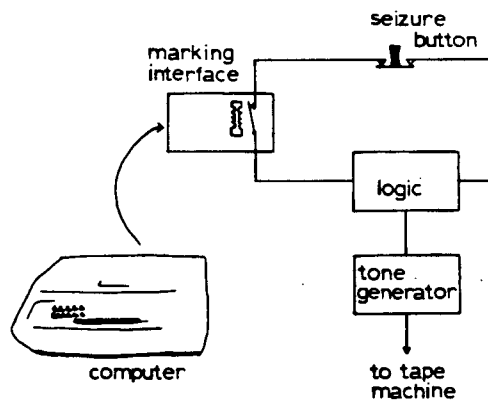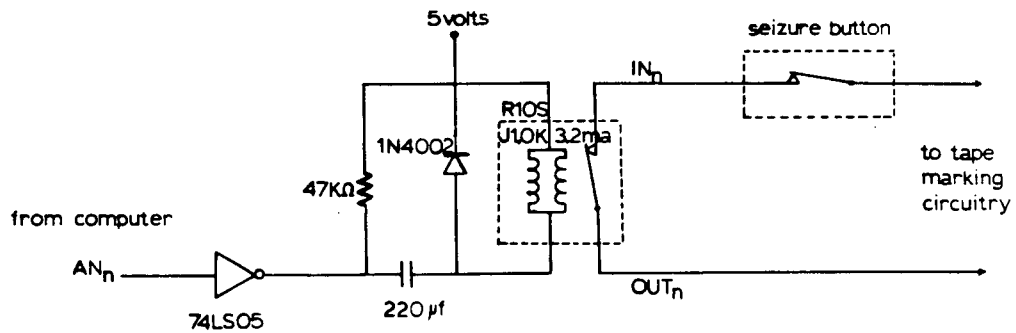

Figure A1 Programmable Timer
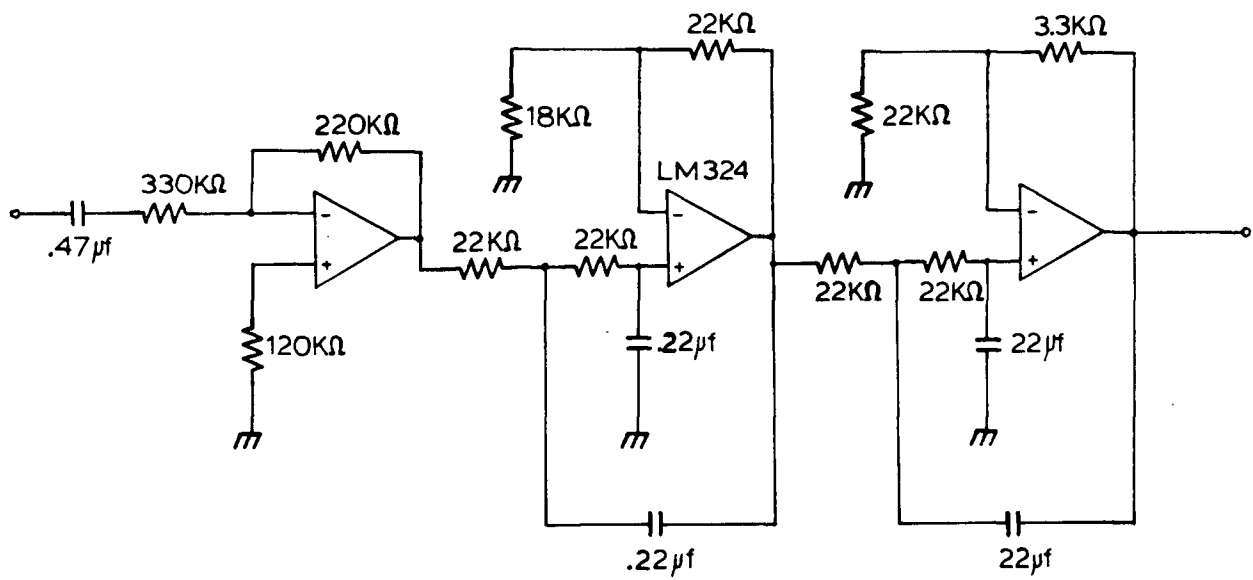
Figure A2 Signal Conditioning Filter

<u>Figure A3</u> Tape marking interface. When a seizure is detected a 10 hz tone is recorded on the audio tape machine which stores the EEG signal.
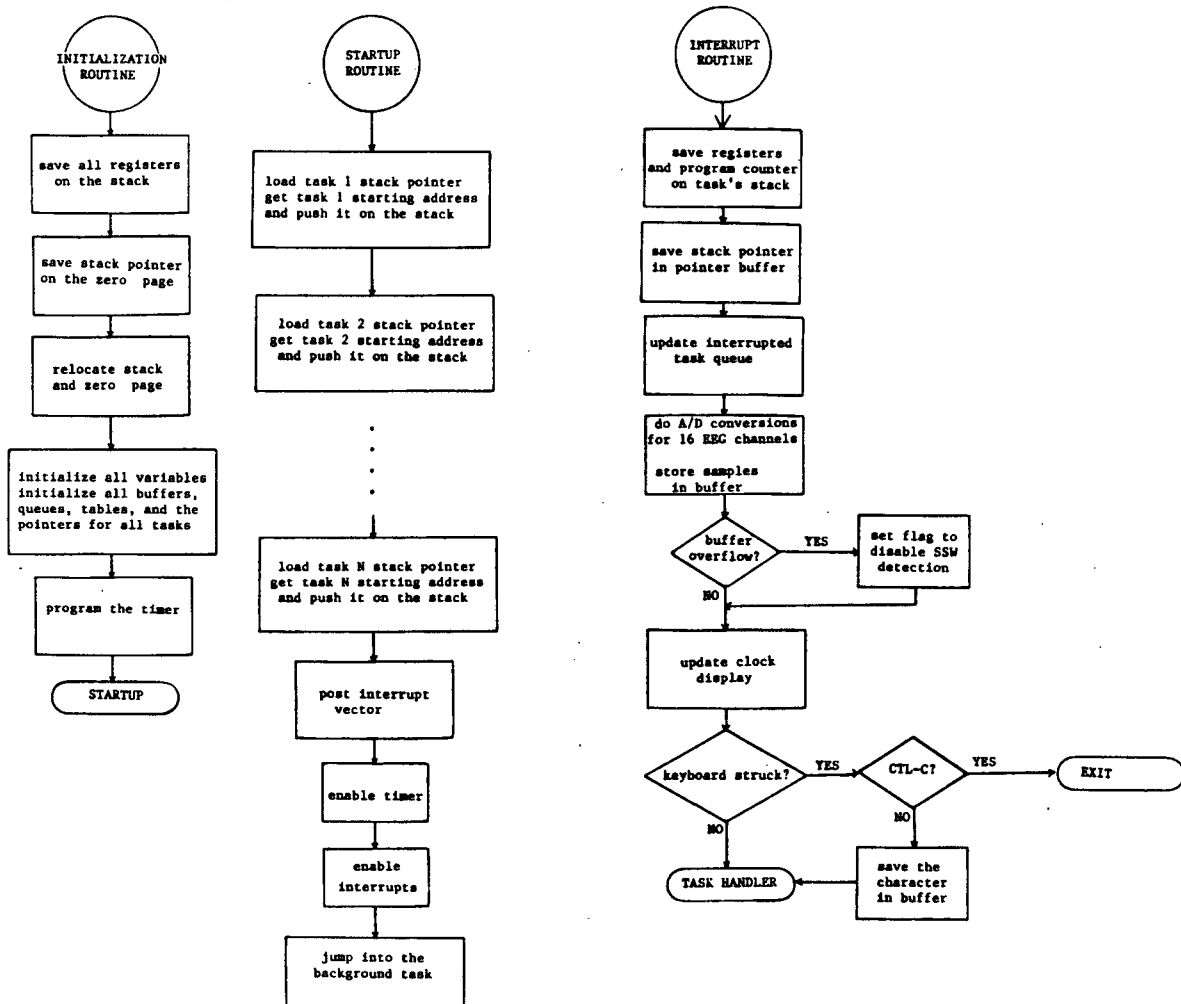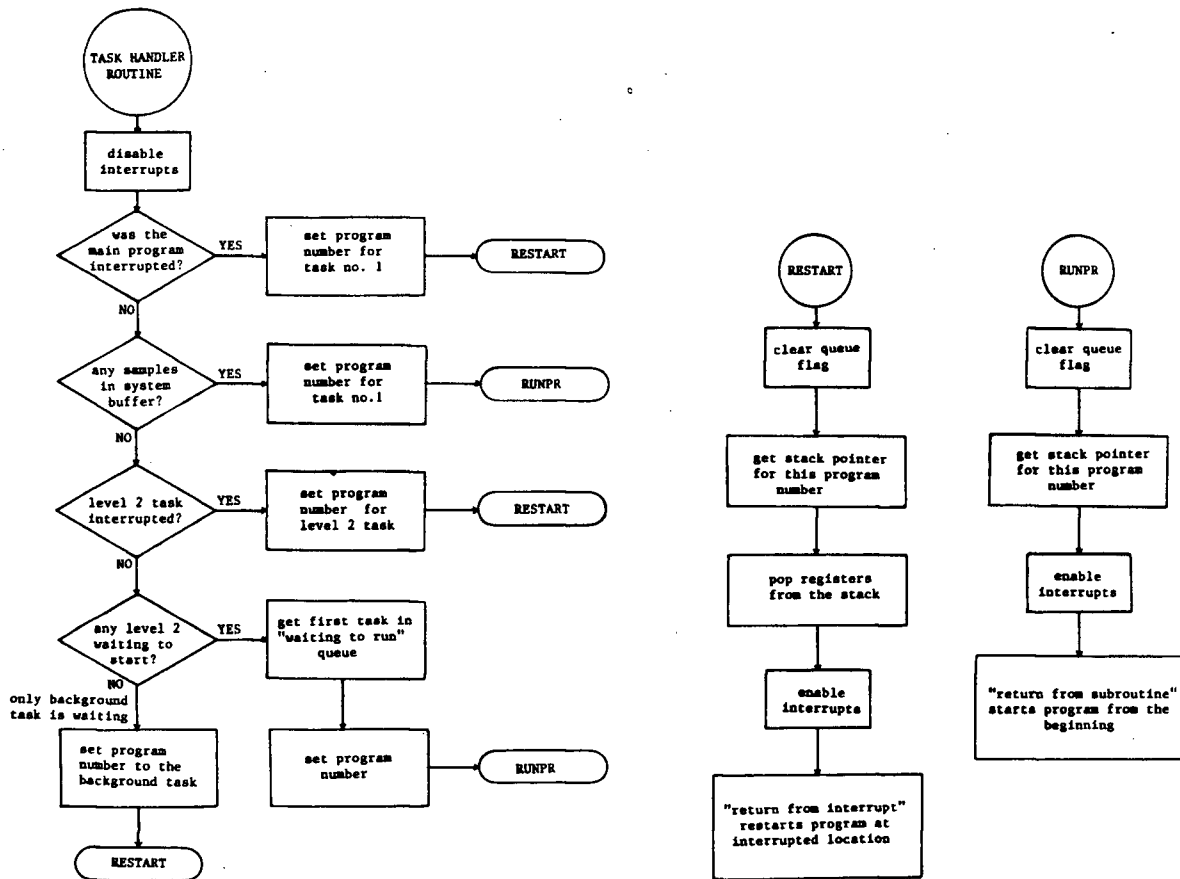
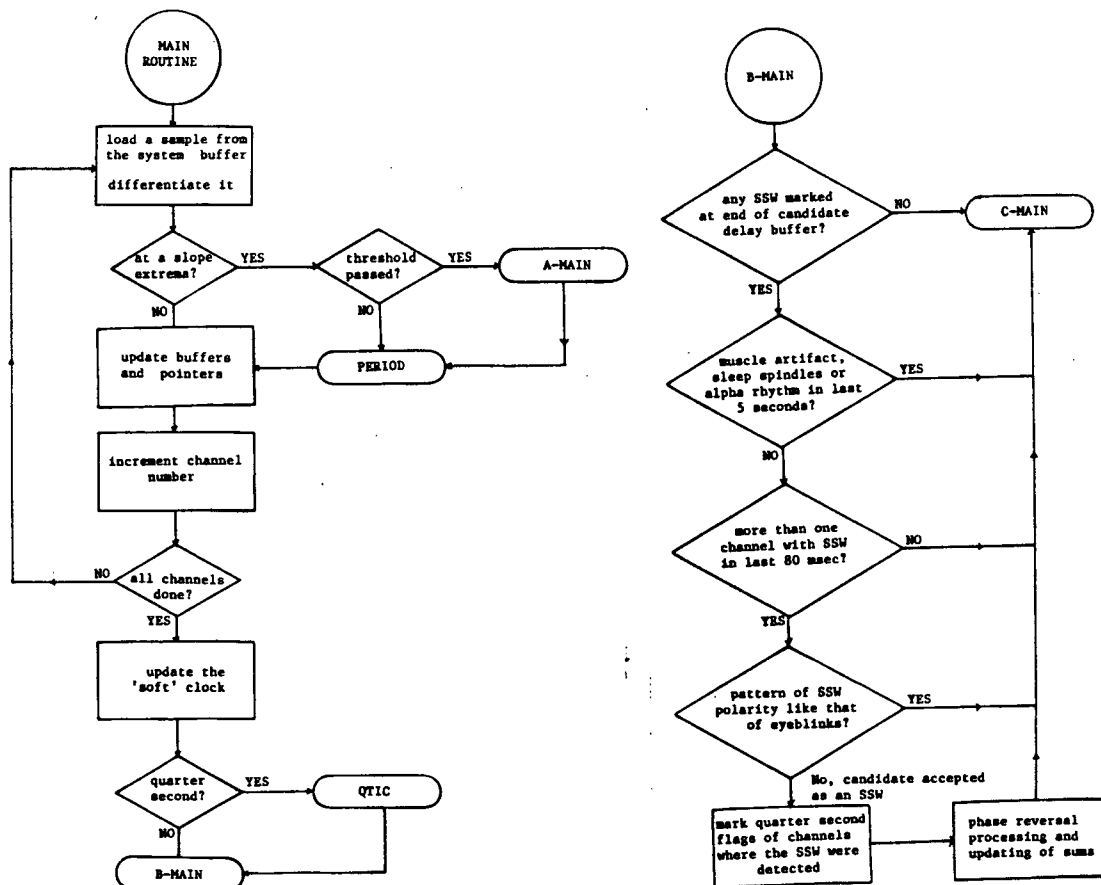# APPENDIX B - INTERICTAL MONITOR SOFTWARE

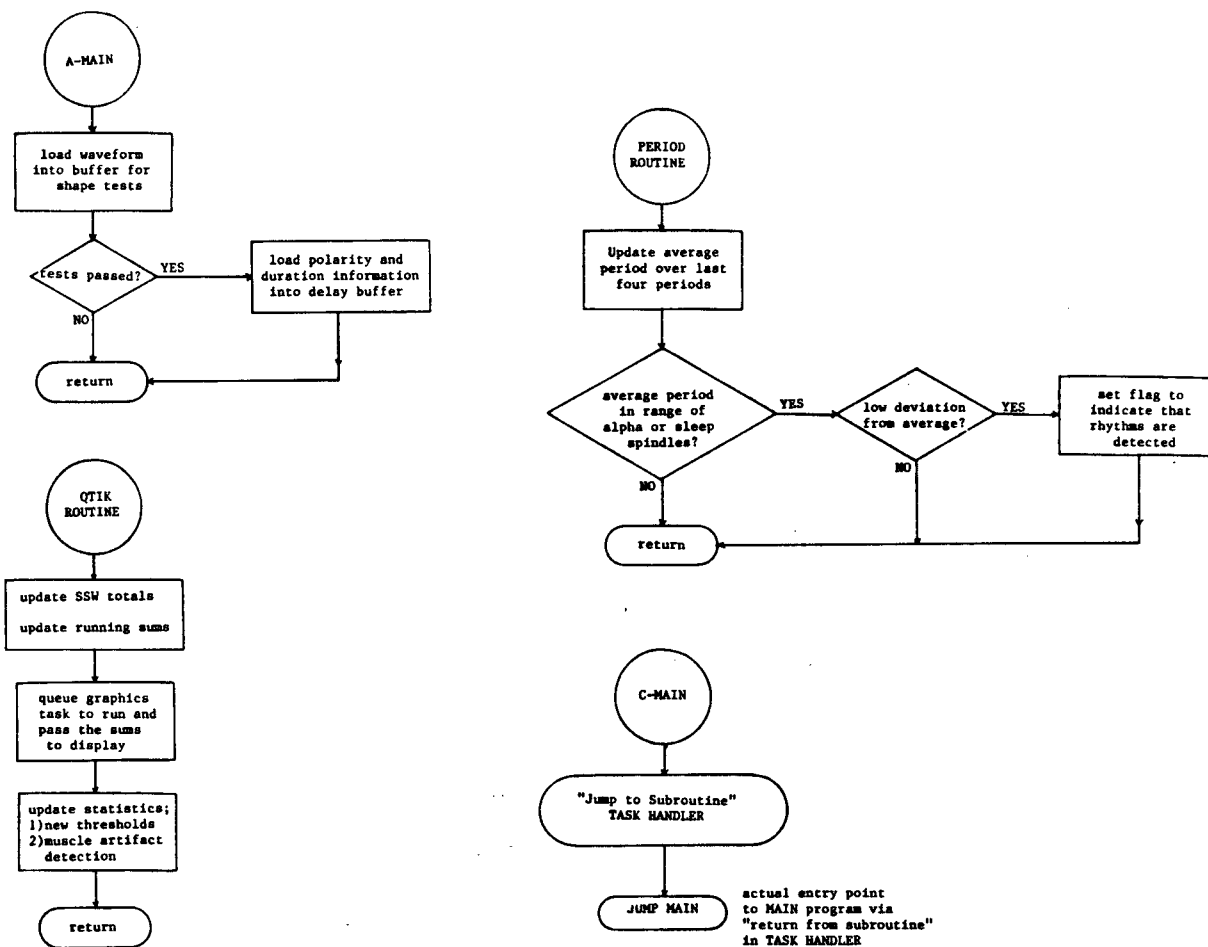**Figure A4** SSW Monitor Software; Initialization, Startup, and Interrupt Routines.

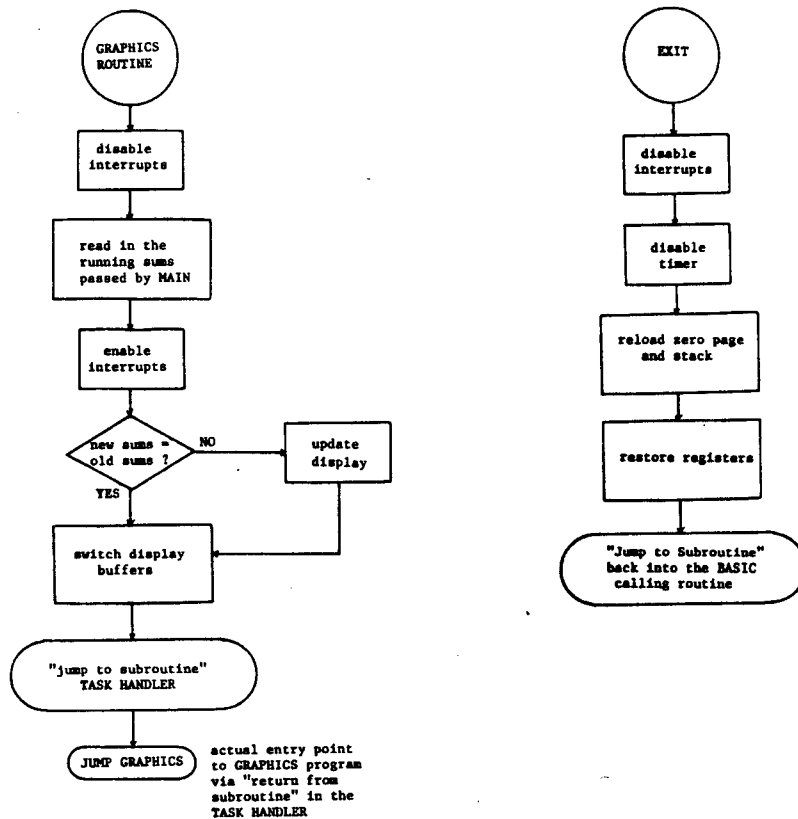**Figure A5** SSW Monitor Software; Task Handler Routines.

Figure A6 SSW Monitor Software; Main Routines.

Figure A7 SSW Monitor Software; Main Routines.

GRAPHICS ROUTINE

- disable interrupts
- read in the running sums passed by MAIN
- enable interrupts
- new sums = old sums ?
  - NO → update display
  - YES
- switch display buffers
- "jump to subroutine" TASK HANDLER
- JUMP GRAPHICS

actual entry point to GRAPHICS program via "return from subroutine" in the TASK HANDLER

EXIT

- disable interrupts
- disable timer
- reload zero page and stack
- restore registers
- "Jump to Subroutine" back into the BASIC calling routine

Figure A8 SSW Monitor Software; Graphics and Exit Routines.